GEMINI NORTH ADAPTIVE OPTICS (GNAO AOB)

“AO bench preliminary optical design”

GEMMA-TPL-001

Related PBS ID: 1.1.2

DRAFT

Document Acceptance and Release Notice
This document is a managed document. To identify changes, each page contains a release number and a page number. This document is authorized for release once all approvals have been obtained and logged in JIRA.

PREPARED:	Emmanuel Chirre Optical Engineering	Date:	03/10/20
APPROVED:	William Rambold GNAO Project Lead Systems Engineer	Date:	
APPROVED:	Manuel Lazo GNAO Project Manager	Date:	
APPROVED:	Gaetano Sivo GNAO Principal Investigator	Date:	
APPROVED:	Henry Roe GNAO Sponsor, Gemini Deputy Director	Date:	

DRAFT

Change Record

Vers.	Date	Description	Change Request	Owner Name
0.1	11/10/20	First Version		E. Chirre
0.2	28/07/21	Rev. 1		E. Chirre

DRAFT

Table of Contents

Applicable Documents 5
Reference Documents 5
Scope 6
Description 6
1. Optical design 8
1.1 Modified Offner Concentric Optical relay 8
1.1.1 Science path 8
1.1.2 Wavefront sensor path 9
1.2 Pair of unmatched Off-Axis Parabolas relay 14
1.2.1 Science path 14
1.2.1 Wave front sensor path 15
1.3 Dimensioning 18
2. Optical Specifications 20
2.1 Modified Offner Concentric relay 22
2.1.1 Science performance 22
2.1.2 WFS performance 27
2.2 Off-axis Parabolas relay 33
2.2.1 Science Performance 33
2.2.1 WFS Performance 37
3. Tolerancing analysis 41
3.1 Modified Offner Concentric relay 42
3.2 Off-axis Parabola relay 43
4. Discussion 45
Acronyms and Abbreviations 47

DRAFT

Applicable Documents

Applicable Documents are those documents containing information that is considered binding in the context of this document. Unless otherwise specified, the latest version of the Applicable Document shall be used. In case of conflict between an Applicable Document and this document, this document shall take precedent.

	Document #	Title	Vers
[AD-01]	Zemax file	GLAO_modifiedOffnerConcentricRelay_sciencePath	
[AD-02]	Zemax file	GLAO_modifiedOffnerConcentricRelay_NGSPath	
[AD-03]	Zemax file	GLAO_modifiedOffnerConcentricRelay_LGSPath	
[AD-04]	Zemax file	GLAO_modifiedOffnerConcentricRelay_science_NGS_LGS	
[AD-05]		GLAO_OAPRelay_sciencePath	
[AD-06]	Zemax file	GLAO_OAPRelay_sciencePath_NGSPath	

Reference Documents

Reference documents are those documents that are included for information purposes only. They may provide additional background or context, but are non-binding in the context of this document.

	Document #	Title	Vers
[RD-01]			
[RD-02]			
[RD-03]			

DRAFT

Scope

This document presents the preliminary design of a Ground Layer Adaptive Optics (GLAO) instrument for the Gemini North Telescope. Two possible optical layouts based on an Offner relay and an OAP relay are studied. Optical specifications in the NIR and the VIS are compared in the aim to determine which one of the two concepts brings the best compromise in terms of performance/benefit ratio. This work does not provide a definitive optical design but tries to give a possible direction to follow regarding the future development of the AO bench for the GNAO project.

Description

The AO bench shall deliver a diffraction-limited image quality in the NIR domain from 0.83 to 2.5um over a 2 arcmin field-of-view to feed GIRMOS (Gemini Infrared Multi-object Spectrograph) the new visitor/facility-class instrument at Gemini North Telescope. The AO bench shall deliver a near diffraction-limited image quality in the VIS domain from 0.45 to 0.83um to feed the laser and the natural wave front guiding systems with the capability to switch between GLAO and LTAO with a reconfigurable LGS WFS.
A common approach to implement an AO instrument is illustrated in Figure 1 with optical relays. On the top left a pair of matched off-axis parabolas (OAP) and on the top at right a combination of three spherical mirrors called Concentric Offner relay. The OAP relay re-images the input f/16 focal plane and produces, in collimated space, an optical plane in which a deformable mirror is placed. OAP produces excellent image quality on-axis but does not balance third-order aberrations off-axis that results in a limitation for the instrument field-of-view.

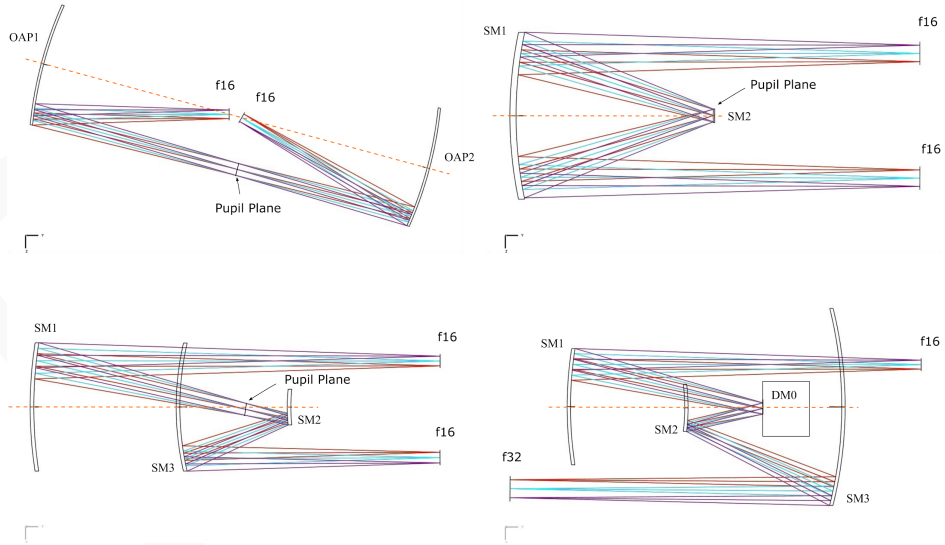

Figure 1: Optical design concept for AO instrumentation. Top, left: OAP relay, a typical approach; Top, right: Offner Concentric relay; Bottom, left: Modified Offner Concentric relay with a unit magnification and accessible optical plane; Bottom, right: Modified Offner Concentric relay with an optical magnification of 2 similar to the pair of unmatched OAP relay for CANOPUS, the MCAO instrument at GS.

Static distortion and Petzal field curvature in an OAP relay are the main contributor to the degradation of off-axis performance while it should be as low as possible to achieve astrometry

requirements. The Offner Concentric relay can produce a very good image quality thanks to a better balancing of third-order aberrations than the OAP relay. By rearranging the optics and the power distribution such that the Petzval sum remains Zero, the pupil plane can be rendered to an accessible location for a DM. The Modified Offner Concentric (MOC) relay is shown in Figure 1 on the bottom at left with an accessible pupil plane. The balancing of Petzval field and third-order aberrations at the image plane is the major benefit in terms of performance compared to OAP relay with the advantage of a wider field-of-view. Figure 1 on the bottom at right, shows the MOC relay with an optical magnification of 2 that is similar to the pair of unmatched OAPs in CANOPUS, the MCAO instrument at GS. The main drawback of such a relay is the lack of collimated space that may be problematic for the refractive optics. A variant of the MOC relay producing a system free of third order aberration is called a three-mirror anastigmat (TMA).

In this document section 1 shows the optical layouts of the science path and wave front sensor path for both designs based on a MOC and OAP relay. Section 2 reviews the optical specifications and performance of each model. Section 3 provides a tolerancing analysis and section 4 discusses the advantages and drawbacks of both concepts for the design of the GLAO optical bench.

DRAFT

1. Optical design

1.1 Modified Offner Concentric Optical relay

1.1.1 Science path

Figure 2 below shows the possible optical layout of the science path based on a Modified Offner Concentric (MOC) optical relay. The f/16 telescope beam is reflected by the AO fold mirror to the optical bench through the AO port of the Instrument Support Structure (ISS) producing a focal plane where the Calibration Source (see red box called Cal.Source) is located. The light is reflected by a fold flat mirror, FM, to the MOC relay. The MOC relay consists of 2 concave spherical mirrors (SM1/SM3) and 1 convex mirror (SM2) that re-images the f/16 focal plane to the f/32 science focal plane with an optical magnification of 2. The MOC relay produces a telecentric beam of 2 arcmin diameter with very good image quality in the NIR domain (see Section 2.1 about MOC optical performance).

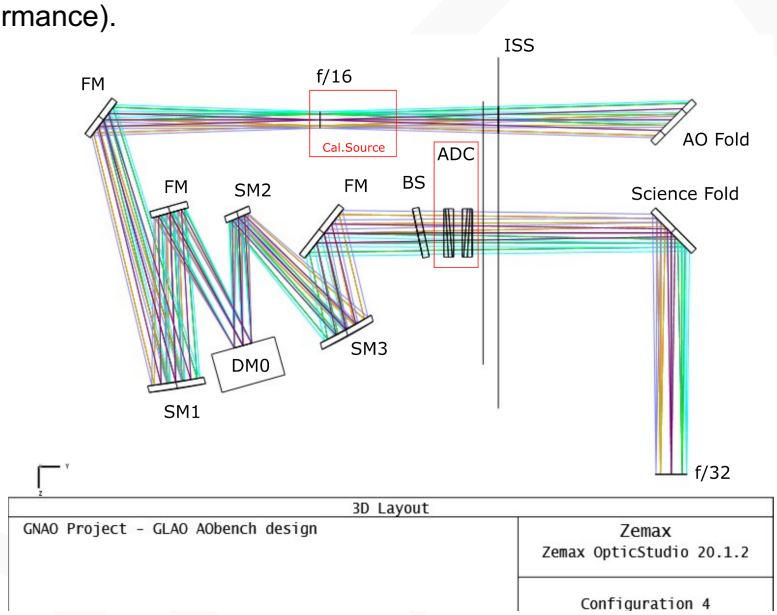

Figure 2: Science optical Layout based on a Modified Offner Concentric optical relay. FM: Fold Mirror; SM: Spherical Mirror; BS: Beam Splitter or dichroic; ADC: Atmospheric Dispersion Corrector; DM: Deformable Mirror; ISS: Instrument Support Structure.

The power distribution is arranged such that the Petzval sum remains zero at the image plane and the optical plane conjugated to the telescope pupil (The secondary mirror) is rendered to an accessible location for the deformable mirror (DM0). The pupil size on the deformable mirror is 85 mm diameter (See Figure 3). No tip-tilt mirror is placed in the optical path assuming DM0 or can provide tip-tilt correction. To achieve the highest throughput and considering the limited space the number of optical components in the optical train is minimized. This preliminary concept does not allow to re-conjugate DM0 to a higher altitude layer with the implementation of an Adaptive Secondary Mirror (ASM).

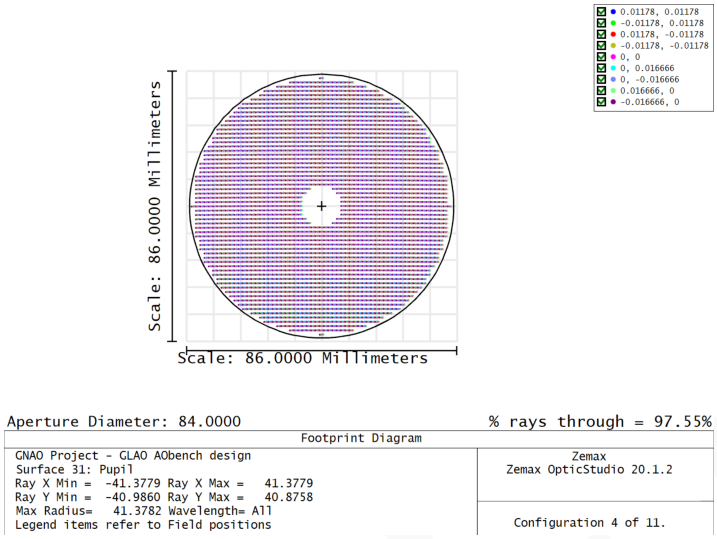

Figure 3: Pupil diameter on the ground deformable mirror DM0.

At the exit of the MOC relay, a fold flat mirror reflects the light to the science Beam Splitter (BS) and the science focal plane through the Science port of the ISS. The BS transmits the NIR and reflects the Visible to the laser and natural wave front sensor. A science Atmospheric Dispersion Corrector (ADC) is located after the BS to correct refraction introduced by the atmosphere at a telescope Zenith angle up to 50 degrees. The science ADC is deployable and can be removed from the optical path when it is not required (See red box called ADC) as it affects throughput. A pair of prisms, called AMICI prisms, are used for simplicity and to optimize glass transmission in the NIR from 0.83 to 2.5um.

1.1.2 Wavefront sensor path

Figure 4 shows the optical layout and a possible optical arrangement of the Natural Guide Star (NGS) and the Laser Guide Star (LGS) in the MOC configuration. The WFS is not shown for readability and the optical path is shown to the focal plane only. In the VIS, the laser light is reflected by the BS while the visible is transmitted. A fold mirror reflects the visible light to the VIS ADC and the NGS WFS. A possible location for the NGS WFS and the LGS WFS is shown in the blue boxes.

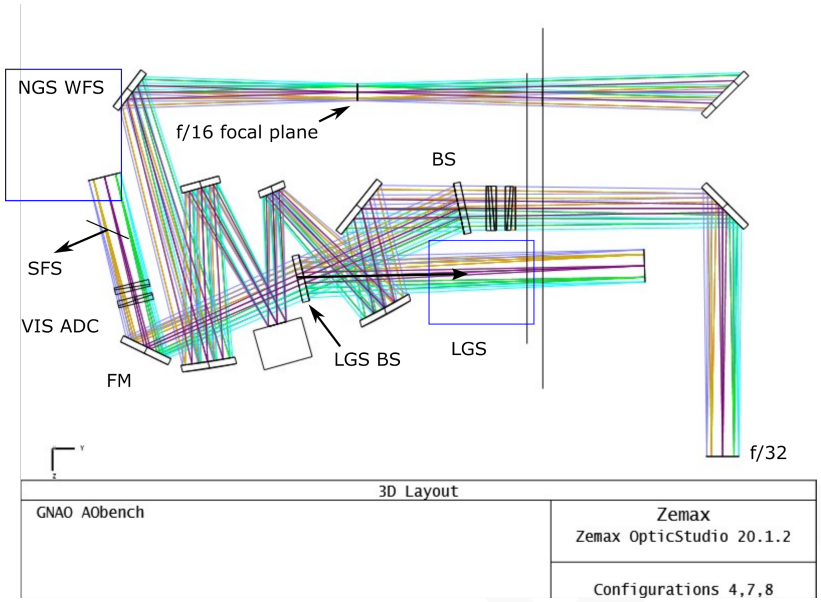

Figure 4: WFS Optical layout. Science path, NGS path and LGS path are shown. WFS is not shown for readability.

The conceptual design of the NGS ADC is also based on a pair of doublet AMICI prisms to optimize throughput (See Figure 5). The NGS ADC is not deployable and cannot be removed from the optical train. The pair of prisms are made of glass with high transmission T>0.98 in the VIS from 0.45 to 0.83um.

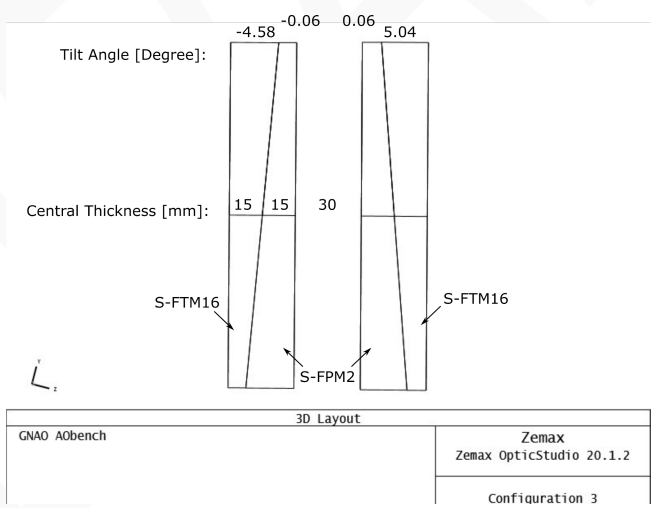

Figure 5: NGS ADC optical layout based on a pair of doublet AMICI prisms.

Figure 6 shows a possible optical layout of the Slow Focus Sensor (SFS). The SFS design is based on a Shack-Hartmann wavefront sensor. It is placed after the VIS ADC. It consists of a converging doublet producing a telecentric focal plane where a square field stop is located. After the stop, a collimating doublet produces an optical plane of 4mm diameter in collimated space conjugated to the telescope pupil in which a Micro-Lens Array (MLA) is placed. A relay lens re-images the lenslet focal plane on a CCD detector with the required dimensions.

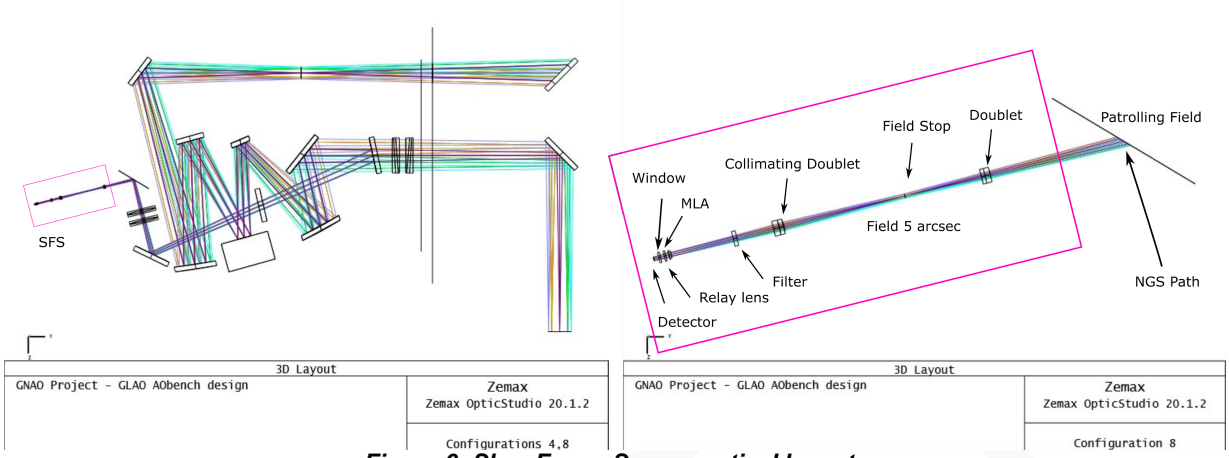

Figure 6: Slow Focus Sensor optical layout.

In order to pick-off the light from a Star in the field, a pick-off mirror patrolling the NGS field is needed. Figure 7 shows a 10X10 illuminated MLA at left and the respective spot diagram on the detector at right in the VIS. The SFS can be also used for calibration purposes.

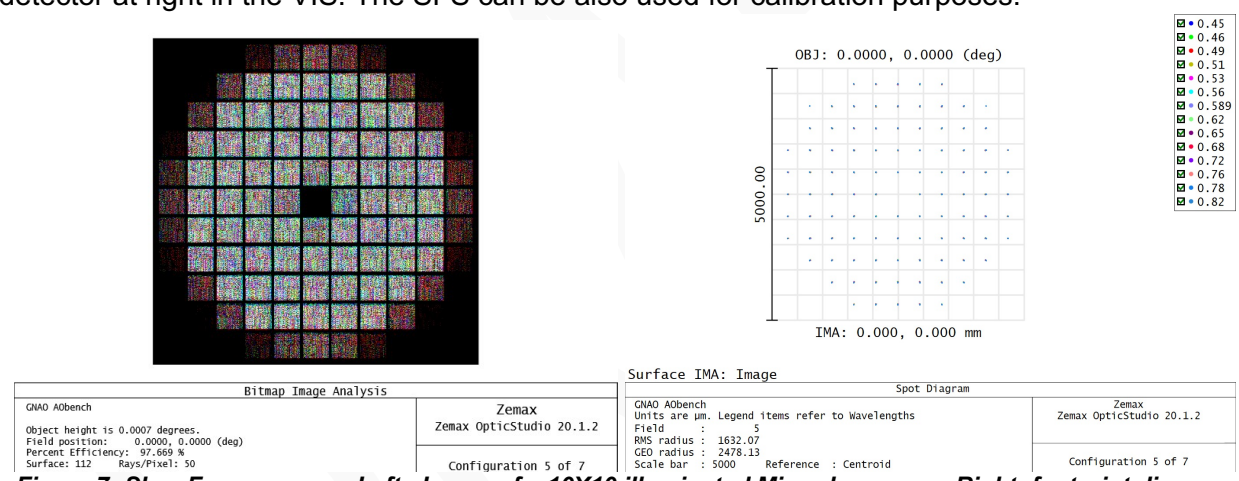

Figure 7: Slow Focus sensor. Left: Image of a 10X10 illuminated Micro-lens array. Right: footprint diagram showing the central spot of each MLA.

Figure 8 shows the possible optical layout of the LGS path for two sodium altitude layers at 85km and 200km. The shape of the LGS constellation for GLAO is a square of 120 arcsec diameter. A trombone system composed of two mirrors facing each other at 45 degrees moves in translation to compensate for the focus shift introduced at different sodium altitudes. The location of the LGS WFS can be problematic due to the little space and a two-level configuration is considered.

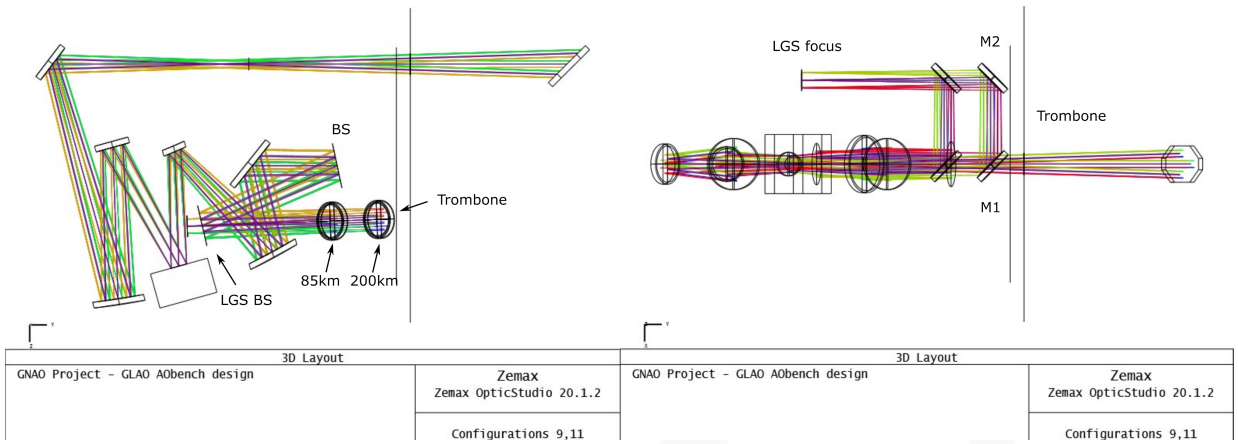

Figure 8: LGS optical layout. Left: Top view. Right: Lateral view.

The LGS WFS layout consists of a common zoom optical system, a pyramid and 4 individual Shack-Hartmann WFS (see Figure 9). The Zoom optics system consists of three groups of lenses in which the intermediate group 2 moves in combination to the trombone. The moving elements maintain the performance at the LGS focal plane and keep the pupil position and size constant on the MLA independently of the sodium altitude, varying from 85km to 200km.

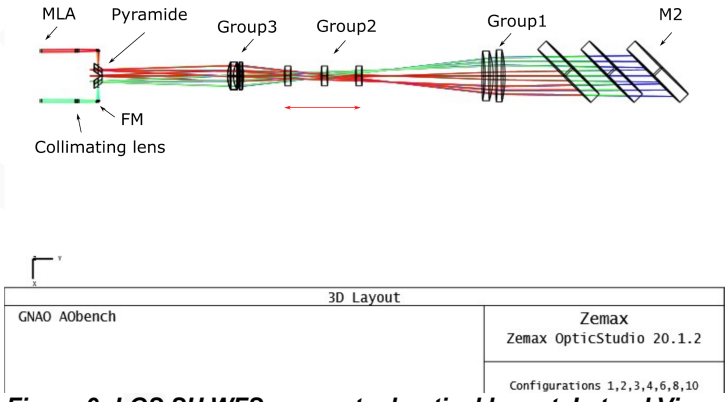

Figure 9: LGS SH WFS conceptual optical layout. Lateral View.

A pyramide is used to separate the 4 LGS beams. The pyramide moves in translation to maintain the LGS focus at the same location when switching between GLAO to LTAO modes. After the Pyramid a fold mirror reflects the LGS beacon to a collimating lens that produces an optical plane in collimated space for the MLA. The LGS system has 3 components moving in translation, the trombone, the group of lens 2 and the pyramid.

DRAFT

1.2 Pair of unmatched Off-Axis Parabolas relay

1.2.1 Science path

Figure 10 shows the possible optical layout of the Science path based on a pair of unmatched Off-Axis Parabolas relay. CANOPUS OAP relay is used as a baseline for the layout and has been re-optimized to minimize the number of components and static distortion at the science focal plane. The f/16 beam is reflected by the AO fold mirror to the optical bench through the AO port of the ISS where the Calibration Source (see red box called Cal.Source) is placed. The light is reflected by a fold flat mirror, FM, to the first OAP (OAP1) of the off-axis relay. The OAP relay consists of a pair of unmatched off-axis parabolas (OAP1 and OAP2) that re-images the f/16 focal plane to the f/32 science focal plane with an optical magnification of 2. The OAP relay produces a telecentric beam of 2 arcmin diameter with good image quality in the NIR domain (see Section 2.2 optical performance).

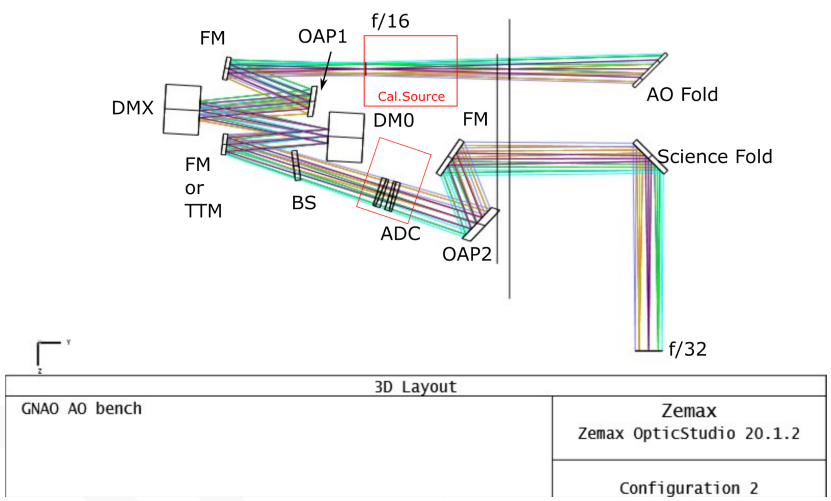

Figure 10: Science optical Layout based on a Off-Axis Parabola (OAP) optical relay. FM: Fold Mirror; OAP: Off-axis parabola; BS: Beam Splitter; ADC: Atmospheric Dispersion Corrector; DM: Deformable Mirror; TTM: Tip-Tilt Mirror; ISS: Instrument Support Structure.

The pupil size on the deformable mirror is 85 mm diameter (See Figure 11). This concept allows to re-conjugate DM0 to a higher altitude layer (DMx) if needed with the implementation of an ASM. Without ASM, DMx is a fold flat mirror. A tip-tilt mirror (TTM) is placed in the optical path after DM0 and it folds the science beam to OAP2. To achieve the highest throughput in the NIR and the need to fold the science path, the number of optics in the optical train is minimized.

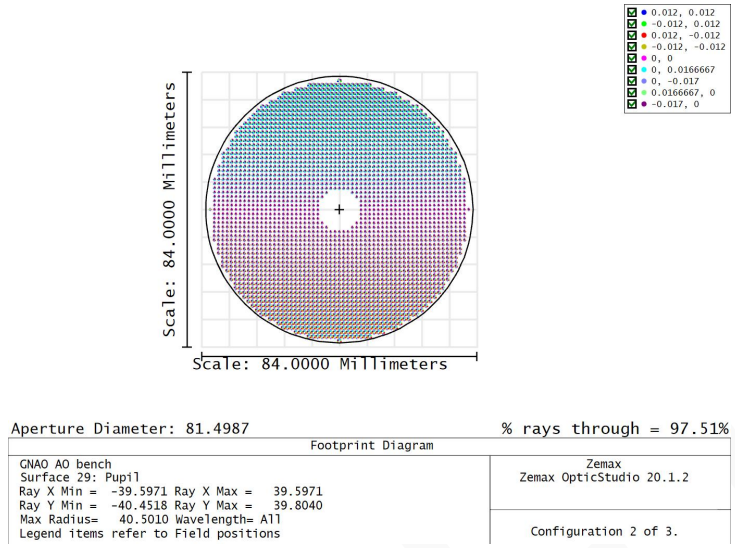

Figure 11: Pupil diameter on the ground deformable mirror DM0.

After the TTM, a BS transmits the NIR to the science and reflects the VIS light to the NGS and the LGS wave front sensor. It is followed by the science ADC. The two refractive elements are placed in collimated space between the two OAPs. The deployable science Atmospheric Dispersion Corrector (ADC) can be moved out of the path when it is not required (See red box called ADC) as it affects throughput. The conceptual design of the Science ADC is based on a pair of doublet AMICI Prisms. The pair of prisms are identical for simplicity and made of glass with high transmission T>0.98 in the NIR from 0.83 to 2.5um similar to the doublet AMICI prism shown in Figure 6.

1.2.1 Wave front sensor path

Figure 12 shows the optical layout and the possible arrangement of the NGS and LGS WFS. A possible location for the NGS WFS and the LGS WFS is shown in the blue boxes. The science BS reflects the VIS light to a third OAP (OAP3) that produces a f/18 focal plane for the LGS and NGS path. No collimated space is accessible for the LGS BS and the VIS ADC and they are placed in the converging beam. The VIS ADC is based on a pair of doublet AMICI prisms similar to the design proposed in Figure 6. The ADC is not deployable.

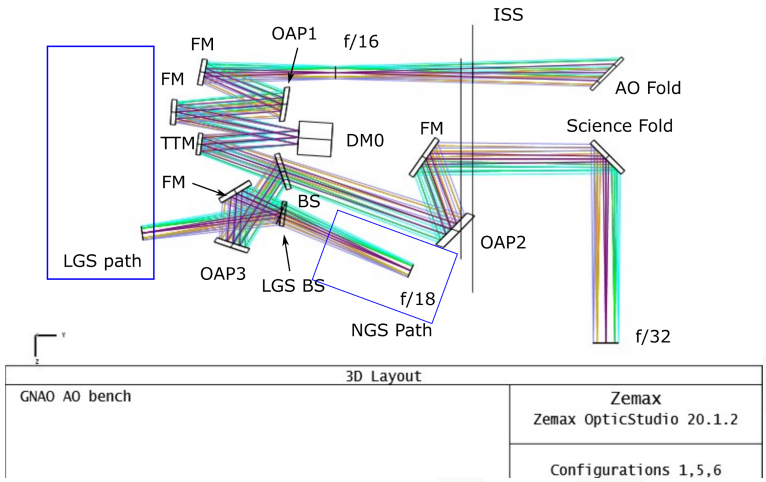

Figure 12: WFS Optical layout. Science path, NGS path and LGS path.

Figure 13 shows the possible optical layout of the LGS path. The folded model shows a trombone system composed of two mirrors facing each other at 45 degrees to compensate for the focus shift at different sodium altitudes. The position of the trombone is illustrated for three cases at 85km, 120km and 200km. The trombone is followed by an optical system that consists of two groups of lenses. The telecentric system re-images the LGS focal plane to meet specifications (telecentricity, centroid location, RMS WFE variation with sodium altitudes) for the individual SH WFS.

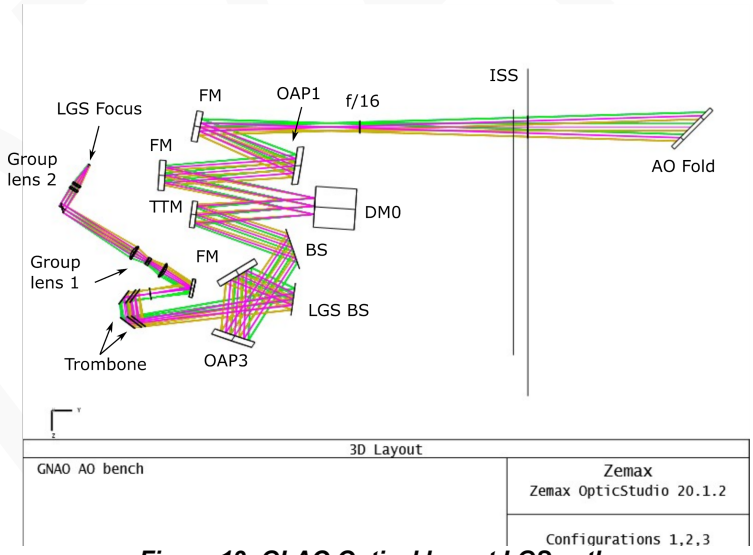

Figure 13: GLAO Optical layout LGS path.

The individual SH WFS is shown in Figure 14. A pyramide near the focal place reflects the light to the SH WFS. The pyramide moves in translation to switch between the GLAO and LTAO mode. The individual SH WFS consists of a field stop, and an afocal telescope in which a mirror is placed

(at an optical plane conjugated to the telescope pupil) to fold the system at 45 degree. A piezo-mirror can be used to maintain the pupil location constant on the Micro-lens Array. A collimating lens after the afocal telescope produces an optical plane of 4 mm diameter in collimated space for the MLA.

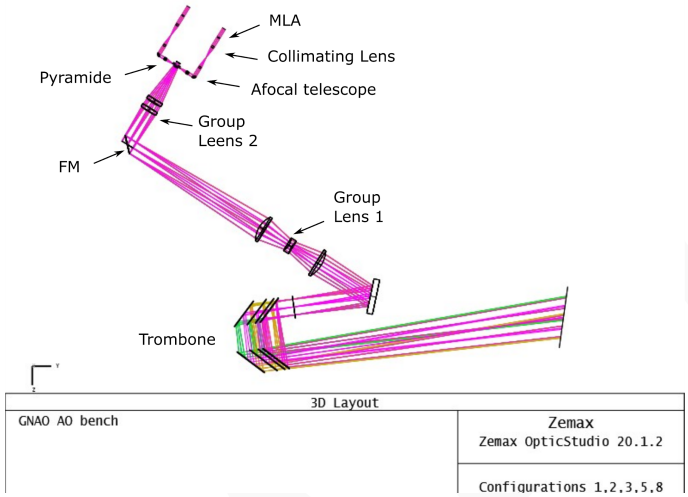

Figure 14: GLAO Optical layout LGS path. Individual Shack-Hartmann WFS.

DRAFT

1.3 Dimensioning

Figure 15 compares the dimension of the MOC relay on the top and the OAP relay on the bottom. Science path, LGS path and NGS path are illustrated in the simplest arrangement.

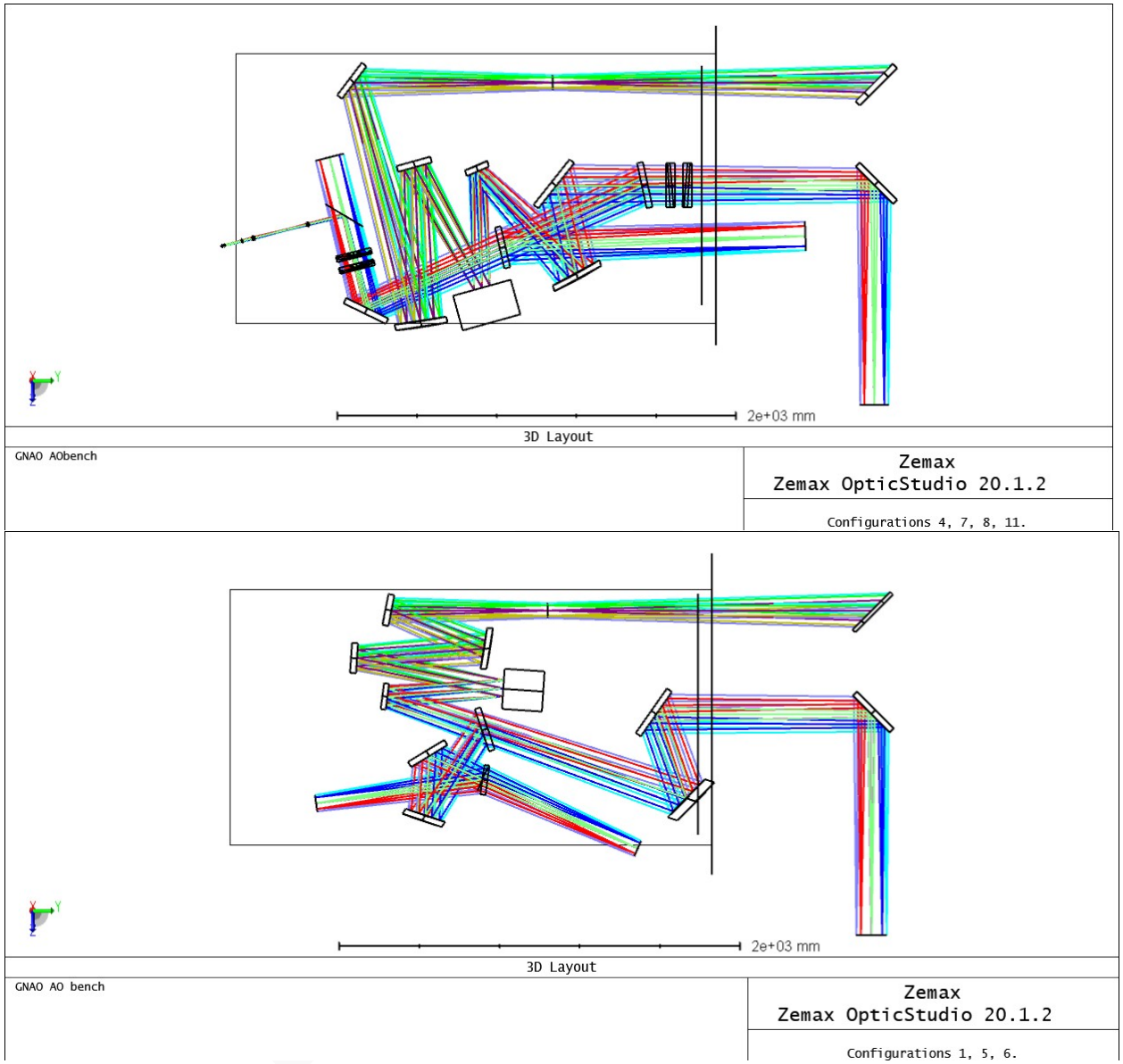

Figure 15: AO bench dimensioning with MOC relay on the top and OAP relay on the bottom.

Figure 15 shows the MOC relay needs more space than the OAP relay and the size of the optics size is bigger. In terms of dimensioning, the OAP relay has the main advantage of being more compact, allowing additional space for the WFS subsystems.

DRAFT

2. Optical Specifications

Table 1, Table 2 and Table 3 show the main optical specifications. Specifications of Table 1 are extracted from the science off-axis optical relay in CANOPUS and specifications of Table 2 are extracted from the WFS off-axis optical relay. Those values are used as a reference for the optical design. The main changes arise from the LGS WFS reconfigurability and the new scope to a GLAO system. For the science and NGS path, the optical specifications will be quite similar to those of CANOPUS. Values may change with the advancement of the project.

Table 1: Science Optical Specifications.

Optical Specifications	AO bench at GS	GNAO GLAO	Unit
Design Baseline	OAP relay	MOC/OAP relay	
Circular Field-of-View diameter	120	120	[arcsec]
Embedded rectangular Field-of-view	85”x85”	85”x85”	[arcsec]
Output Focal Ratio	f/32	f/32	Unitless
Zenith Angle, Zd	45	50	[Deg]
Static maximum distortion	<2	<2, Goal <0.3	[%]
Absolute optical distortion	<TBD	<180	[mas]
Sagittal/Tangential Field curvature	<2/2	<2/2, Goal <1	[mm]
Wavelength Coverage	0.85-2.5 with ADC 0.85-2.5 w/o ADC	0.83-2.5 with ADC 0.83-5.0 w/o ADC	[um]
Throughput@1.65 um	>80	>85	[%]
Strehl ratio @1.65 um	>95 ± 2 on-axis >95 ± 2 off-axis	>95 ± 2 on-axis >95 ± 2 off-axis	[%]
Strehl ratio @2.2 um	>98 ± 2 on-axis >98 ± 2 off-axis	>98 ± 2 on-axis >98 ± 2 off-axis	[%]
Telecentricity	<1000	<1000	[arcsec]
Exit Pupil Position	16.5	16.5	[m]
Conjugate Layer	0 - 4.5 - 9km	0, Goal reconfigurable to 4km	[km]
Chromatic Shift	<0.01	<0.01	[mm]
Lateral Color	<0.01	<0.01	[mm]
Residual Chromatic dispersion	<60	<60	[mas]
Wave Front Error	<60 RMS	Goal <40 RMS	[nm]

Table 2: NGS Optical Specifications

Optical Specifications	AO bench at GS	GLAO design	Unit
Circular Field-of-View diameter	120	120	[arcsec]
Output Focal Ratio	f/16	f/16 < f/# < f/32	Unitless
Zenith Angle, Zd	45	50	[Deg]
Static distortion	<2	<2	[%]
Sagittal/Tangential Field curvature	<1/1	<1/1	[mm]
Wavelength Coverage	0.45-0.95	0.45-0.83	[um]
Throughput@0.6 um	>80	>85	[%]
Strehl ratio @0.6 um	>50 on-axis >50 off-axis	>TBD on-axis >TBD off-axis	[%]
Telecentricity	<1600	<1000	[arcsec]
Chromatic shift	<0.5	<0.05	[mm]
Lateral Color	<0.01	<0.01	[mm]
Residual Dispersion	<50	<25	[marcsec]
Wave Front Error	<100 RMS	<80 RMS	[nm]

Table 3: LGS Optical Specifications

Optical Specifications	AO bench at GS	GLAO design	Unit
Design Baseline	SH WFS	SH WFS	
LGS spots	5	4	
Reconfigurable	No	GLAO to LTAO	
Constellation Shape	Square (4 corners + 1 center)	Square (4 corners)	
Field-of-View diameter	60	100 in GLAO 40 in LTAO	[arcsec]
Output Focal Ratio	f/16	f/16 < f/# < f/32	Unitless
Zenith Angle, Zd	45	50	[Deg]
Sodium altitude	90-200	85-200	[km]
Static distortion	<TBD	<TBD	[%]
Sagittal/Tangential Field curvature	<TBD	<TBD	[mm]
Wavelength Coverage	0.589	0.589	[um]
Throughput@0.589 um	>80	>85	[%]
Strehl ratio @0.589 um	> TBD	>95 off-axis	[%]
MLA	12X12	16X16	sub apertures
Pitch	250	250	[um]
Pupil size variation on MLA	<0.1	<0.1	[mm]

Centroid variation X/Y at each LGS Focus	<0.01	<0.01	[mm]
Pupil position variation on MLA	<0.01	<0.01	[mm]
Telecentricity	<	<1000	[arcsec]
Telecentricity Variation at each LGS focus	<	<300	[arcsec]
Chromaticity	<	<50	[marcsec]
Wave Front Error	<	<120 RMS	[nm]

2.1 Modified Offner Concentric relay

The following section shows the optical performance of the MOC relay in the NIR and the VIS for the science and WFS path, respectively. Optical specifications are provided at the science focal plane in the NIR domain at 1.65um (input for GIRMOS instrument) and at the NGS focal plane in the visible domain at 0.6um (input for the WFS).

2.1.1 Science performance

The following Figures show the optical performance of the MOC relay in the NIR domain at 1.65um. Figure 16 shows the spot diagram over the field-of-view and the static optical distortion. The optical distortion at the science focal plane is <0.5% on average. Figure 17 shows the Point Spread Function (PSF) at 1.65um on-axis and off-axis. PSF is 99% on-axis and 96.6% off-axis with a maximum variation of 2.5% over the field. On average the Strehl ratio is 98% over the entire field.

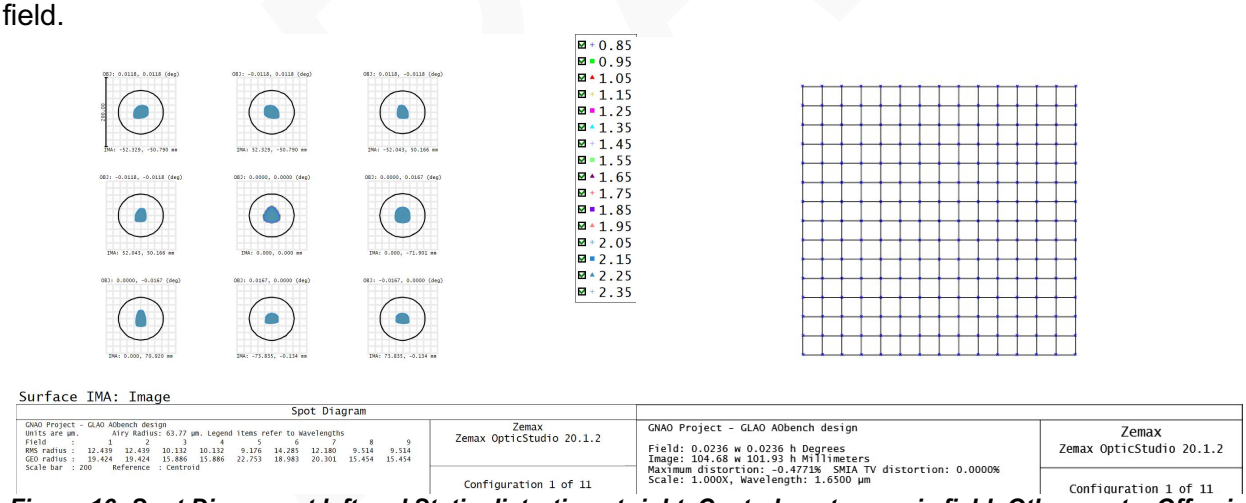

Figure 16: Spot Diagram at left and Static distortion at right. Central spot: on-axis field; Other spots: Off-axis fields at 1 arcmin radius from the center.

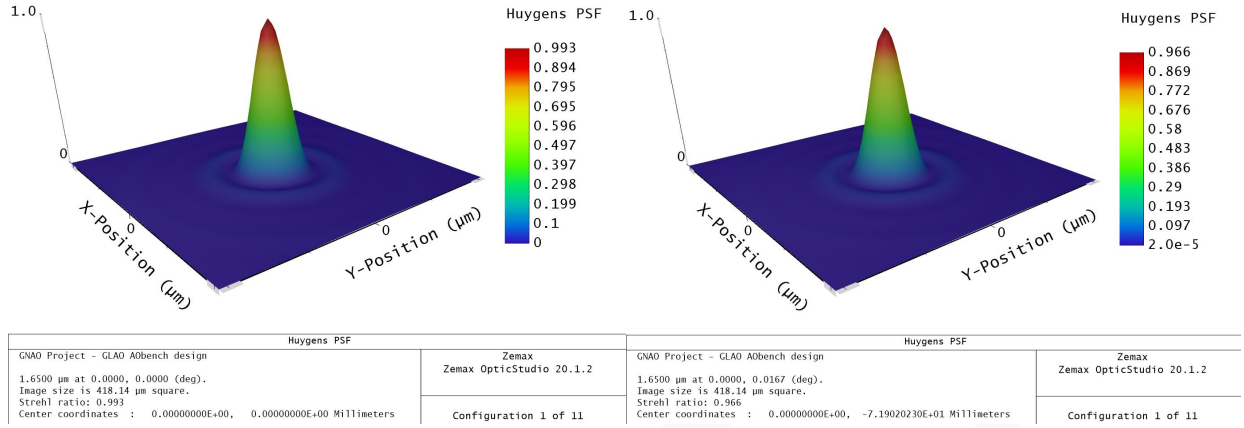

Figure 17: Point Spread Function on-axis at left and for the worst performing field off-axis at right. Strehl ratio is 99% on-axis and 96.6% off-axis.

Figure 18 shows the Sagittal and Tangential field curvature in +Y and +X as a function of the field size. Figure 19 shows the polychromatic RMS WaveFront error in +Y and +X as a function of the field size. In both Figures, performance in -Y and -X are not shown for similarity. It can be seen that Field Curvature is less than 2mm on average at the edge of the field. Regarding RMS WFE error, it is shown the MOC relay is diffraction-limited for all the wavelengths in the NIR domain from 0.83 to 2.5um and over the entire Field-of-view.

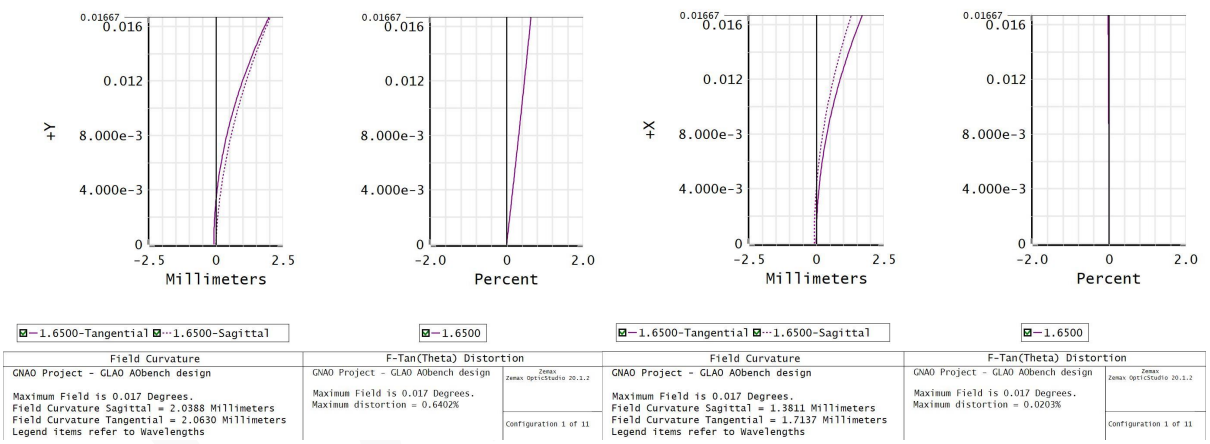

Figure 18: Field curvature. Left: in +Y; right: in +X.

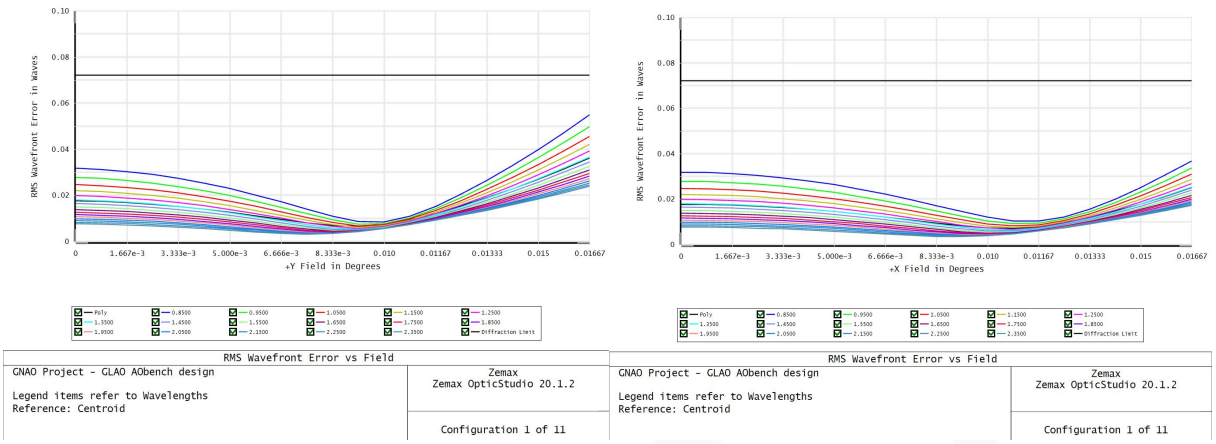

Figure 19: RMS WFE as a function of Field in +Y and +X at left and right. each color for each wavelength. Black line is diffraction-limited.

Figure 20 shows the wave front map for the on-axis field and the worst performing off-axis field at a wavelength of 1.65um. RMS WFE is 22nm on-axis and 49nm off-axis. The requirement of 60nm RMS for wave front error is met over the entire field and the goal of 40 nm can be achieved.

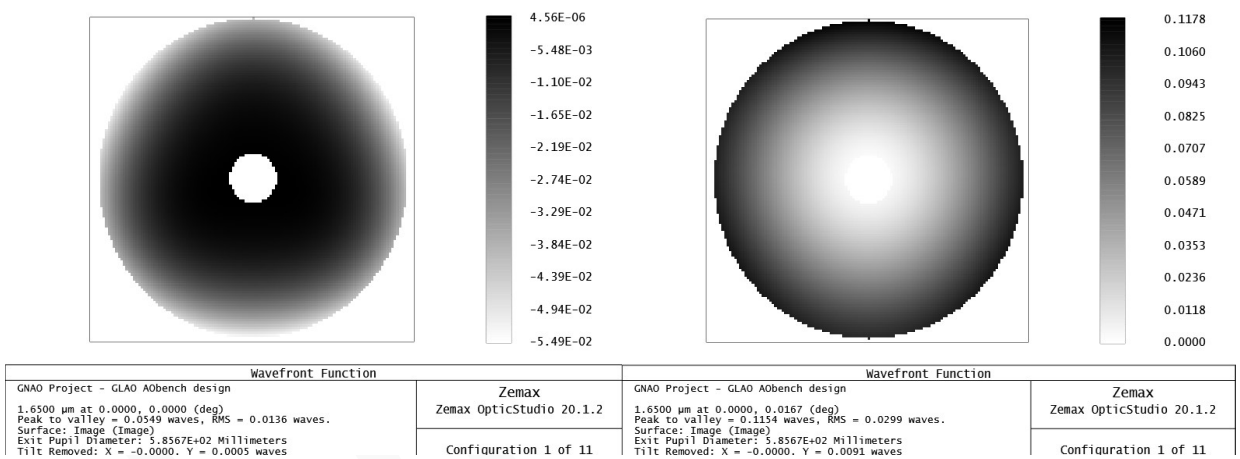

Figure 20: Wave front Map on-axis at left off-axis at right at 1.65um.

The reflective design of the MOC relay does not produce chromatic aberration at the science focal plane. Due to the location of the refractive optics in the converging beam, a slight amount of chromatic aberration is introduced by the science beam splitter. This effect can be minimized by introducing an optical wedge and/or a toroid on the rear surface of the BS. It is also important to limit the tilt angle. The glass material for the BS is SILICA for the high transmittance in the NIR wavelength coverage. Caf2 is a possible glass material alternative for extending wavelength coverage up to 5um. Figure 21 shows the Lateral and Longitudinal color at science focus.

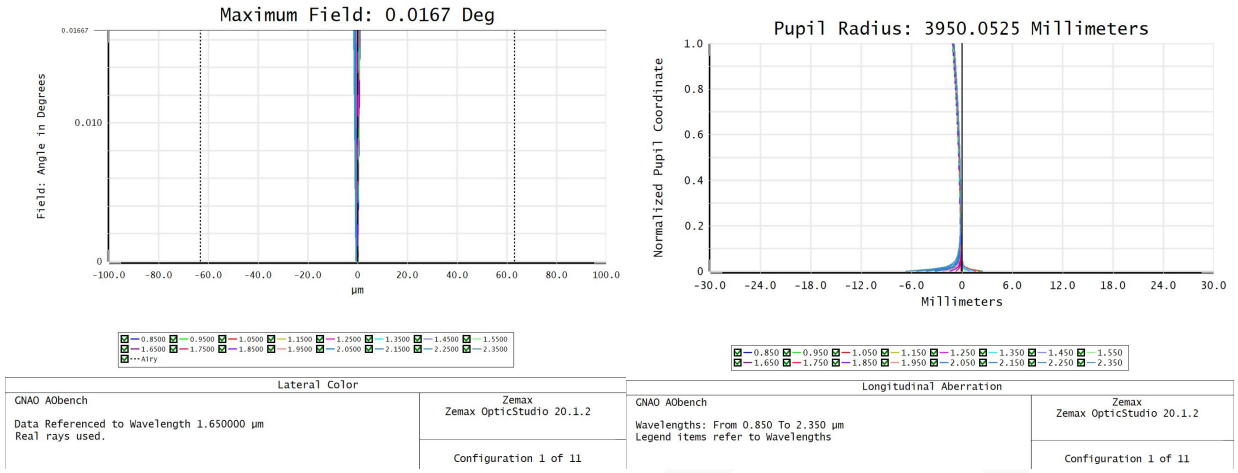

Figure 21: Lateral and Longitudinal aberration as a function of field. each color for each wavelength.

No significant amount of lateral color is seen at the science focal plane. A chromatic shift of 0.288mm from 0.83 to 2.5um is introduced by the BS and cannot be totally cancelled, which means the focal position may vary with wavelengths as shown in Figure 22.

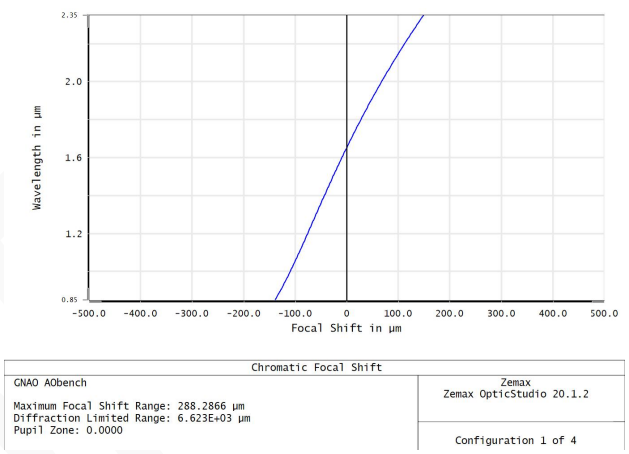

Figure 22: Chromatic shift at the science focal plane as a function of wavelengths in the NIR Domain.

The residual chromatic dispersion at the science focal plane is mainly due to the atmospheric dispersion at different telescope elevations. To counterbalance the effect of atmospheric dispersion, the science ADC rotates along the optical axis. Figure 23 shows the matrix spot diagram and Figure 24 shows the residual chromatic dispersion for three telescope elevations, Zd, at 10Deg. 30Deg. and 55Deg.

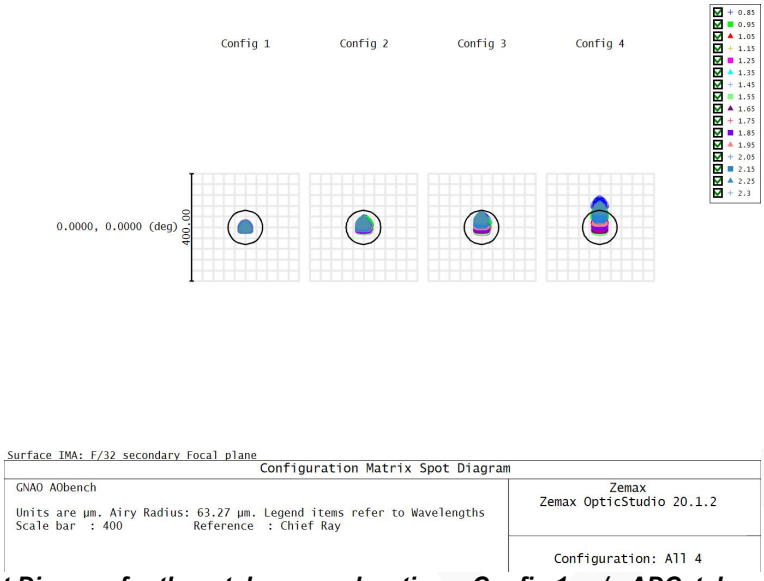

Figure 23: Matrix Spot Diagram for three telescope elevations. Config 1: w/o ADC, telescope at Zenith; Config 2: with ADC telescope elevation, Zd, of 10Deg.; Config 3: with ADC telescope elevation, Zd, of 30Deg.; Config 4: with ADC telescope elevation, Zd, of 55Deg.

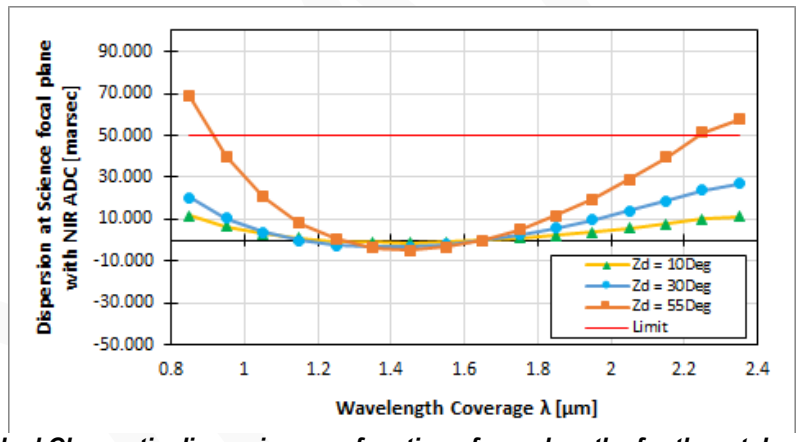

Figure 24: Residual Chromatic dispersion as a function of wavelengths for three telescope elevations. Yellow: Zd 10Deg.; Blue: Zd 30Deg.; Orange: Zd 55Deg.; Red line is the upper limit of 50 marcsec. ADC Rotation angle is 78Deg., 63Deg. and 1Deg.

The estimated throughput of the science path without ADC is 89% at 1.65um with protected silver coating for reflective optics (R ~ 99%) and AR coating for the refractive optics (T ~ 96% for BS). Table 4 shows the throughput calculation without ADC.

Table 4: Science Throughput

number of element	Optics	Coating	T@1.65um	T@2.2um in K-band

1	FM	Protected Silver	99.00	99.00
2	SM1	Protected Silver	99.00	99.00
3	FM	Protected Silver	99.00	99.00
4	DM0	Protected Silver	99.00	99.00
5	SM2	Protected Silver	99.00	99.00
6	SM3	Protected Silver	99.00	99.00
7	FM	Protected Silver	99.00	99.00
8	BS	SILICA + NIR AR Coating	96.00	96.00
9	ADC	NIR GLASS	TBD	TBD
Total	AO bench Science path w/o ADC		89.00	89.00

The optical specifications of Table 1 are met by the MOC relay in the NIR spectral range. The relay is diffraction-limited over the entire field-of-view with a Strehl better than 98% and a variation of PSF about 2%. Distortion is reduced by a factor of 4 compared to the OAP relay in CANOPUS that is a significant improvement for astrometry. The goal of 40nm RMS is also achieved at the science focal plane. The main limitation regarding optical performance is the chromatic shift introduced by the refractive optics due to the lack of collimated space.

2.1.2 WFS performance

The following section shows the optical performance extracted from the MOC relay in the VIS domain at 0.6um for the WFS subsystem. Figure 25 shows the spot diagram over the field-of-view and the static optical distortion. The optical distortion at the NGS focal plane is <0.5% on average. Figure 26 shows the Point Spread Function (PSF) at 0.6um on-axis and off-axis. PSF is 79% on-axis and 96.6% off-axis. As it can be seen, the MOC relay is also performing well in the VIS domain.

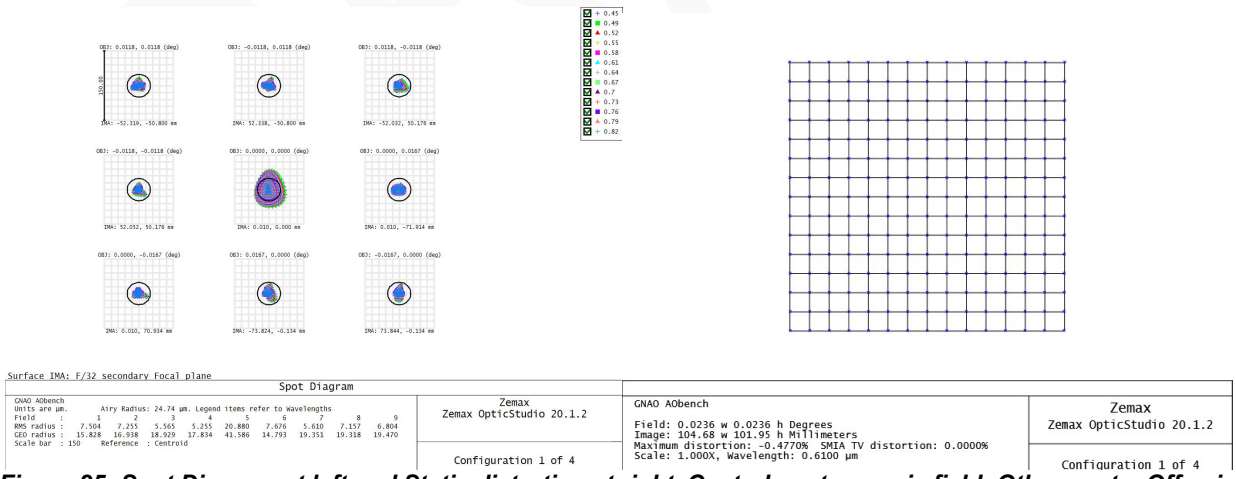

Figure 25: Spot Diagram at left and Static distortion at right. Central spot: on-axis field; Other spots: Off-axis fields at 1 arcmin radius from the center.

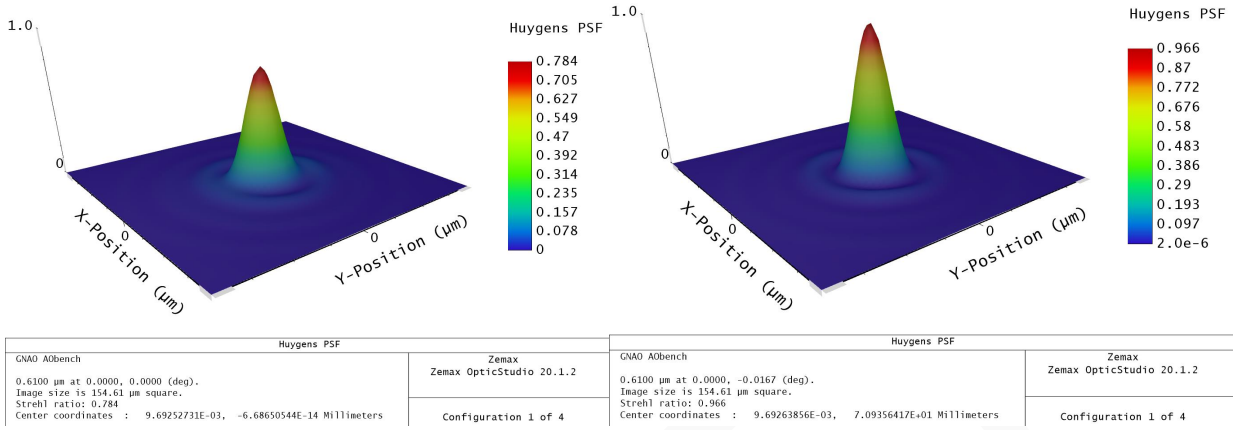

Figure 26: Point Spread Function on-axis at left and for the worst performing field off-axis at right. Strelh ratio is 79% on-axis and 96.6% off-axis.

Figure 27 at left shows the Sagittal and Tangential field curvature in +Y as a function of the field size and Figure 27 at right shows the polychromatic RMS WaveFront error in +Y as a function of the field size. In both Figures, performance in -Y and -X are not shown for similarity. It can be seen that Field Curvature is less than 2mm on average at the edge of the field.

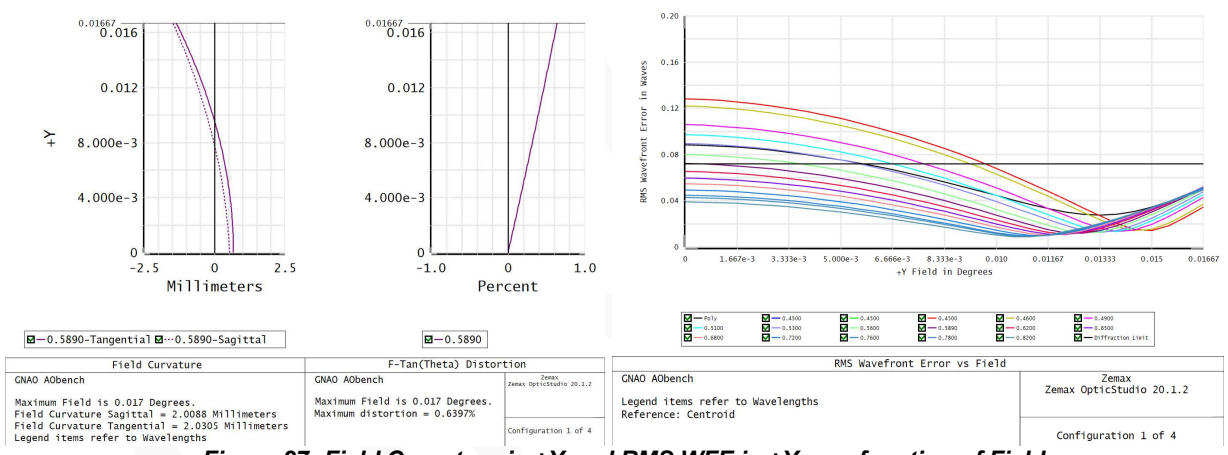

Figure 27: Field Curvature in +Y and RMS WFE in +Y as a function of Field.

Figure 28 shows the wave front map for the on-axis field and the worst performing off-axis field at a wavelength of 0.6um. RMS WFE is 43nm on-axis and 20nm off-axis.

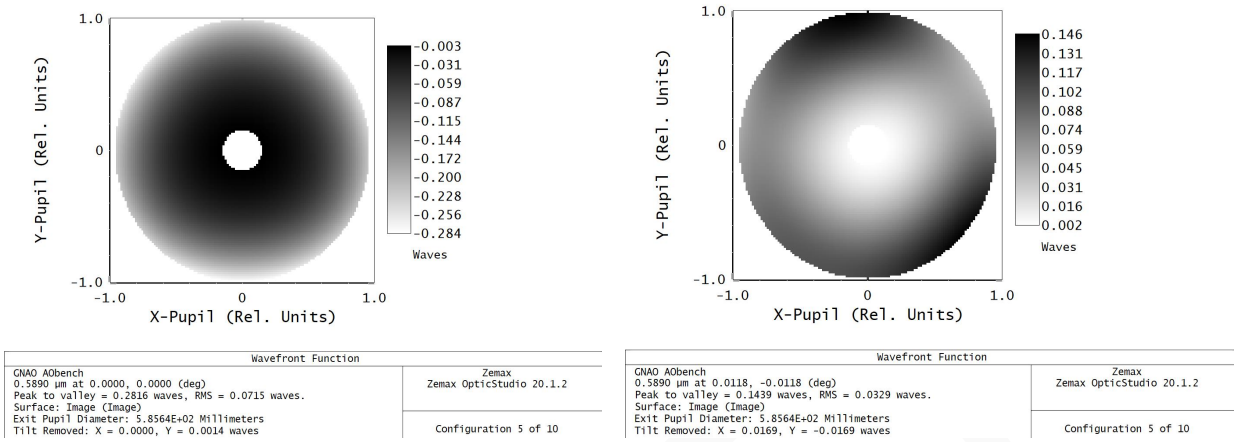

Figure 28: Wave front Map on-axis at left off-axis at right at 0.6um.

The reflective design of the MOC relay does not produce chromatic aberration at the NGS focal plane. The location in the converging beam of the LGS BS produces chromatic aberration. This effect can be minimized by introducing an optical wedge and a toroid on the rear surface of the BS and by limiting the tilt angle. Figure 29 shows the Lateral and Longitudinal color.

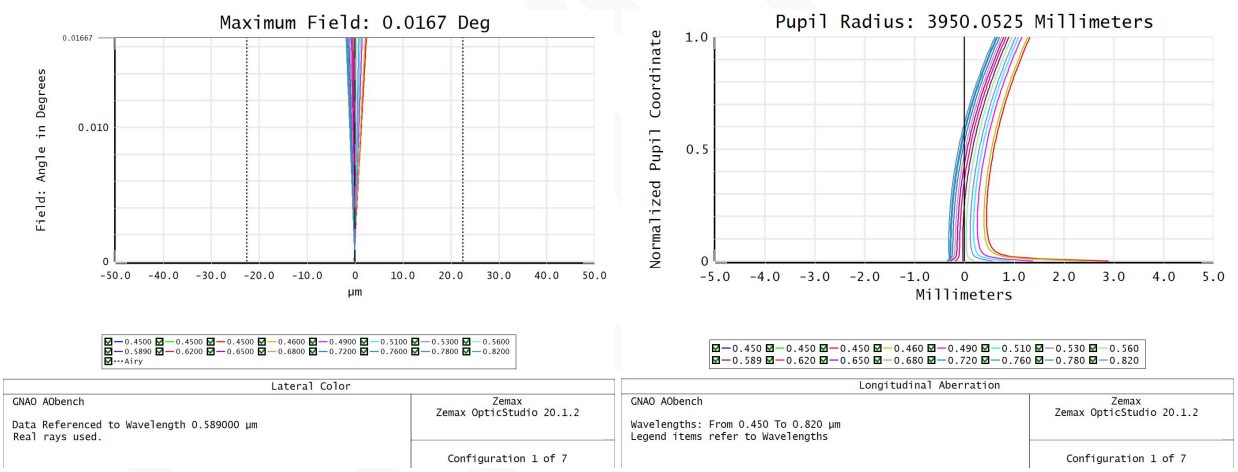

Figure 29: Lateral and Longitudinal aberration as a function of field. each color for each wavelength.

The chromatic aberration produces a chromatic shift of 0.600mm from 0.45 to 0.83um at the NGS focal plane that cannot be cancelled by the optical wedge on the LGS BS. The variation of the focal position with wavelengths is shown in Figure 30.

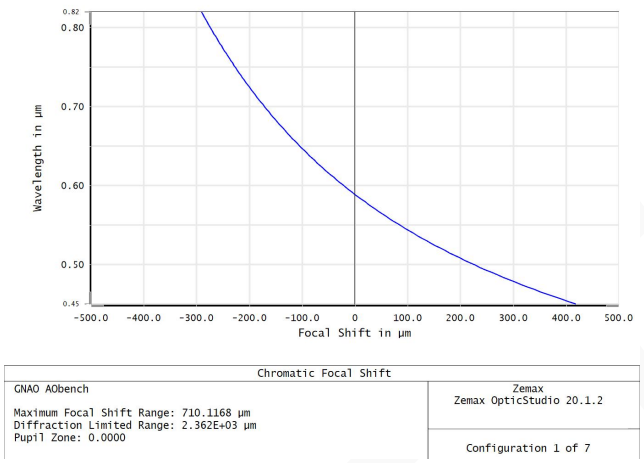

Figure 30: Chromatic shift at the NGS focal plane as a function of wavelengths in the VIS Domain.

The residual dispersion at the NGS focal plane is also due to the effect of atmospheric dispersion at different telescope angles. To counterbalance this effect the doublet prisms of the NGS ADC are rotated along the optical axis. Figure 31 shows the matrix spot diagram and Figure 32 shows the residual chromatic dispersion for three telescope elevations, Zd, at 10Deg. 30Deg. and 55Deg.

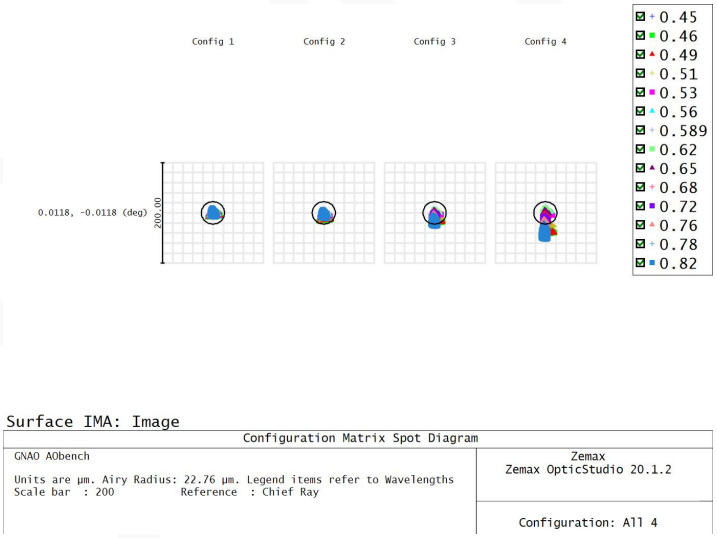

Figure 31: Matrix Spot Diagram for three telescope elevations. Config 1: w/o ADC telescope at Zenith; Config 2: with ADC telescope elevation, Zd, of 10Deg.; Config 3: with ADC telescope elevation, Zd, of 30Deg.; Config 4: with ADC telescope elevation, Zd, of 55Deg.

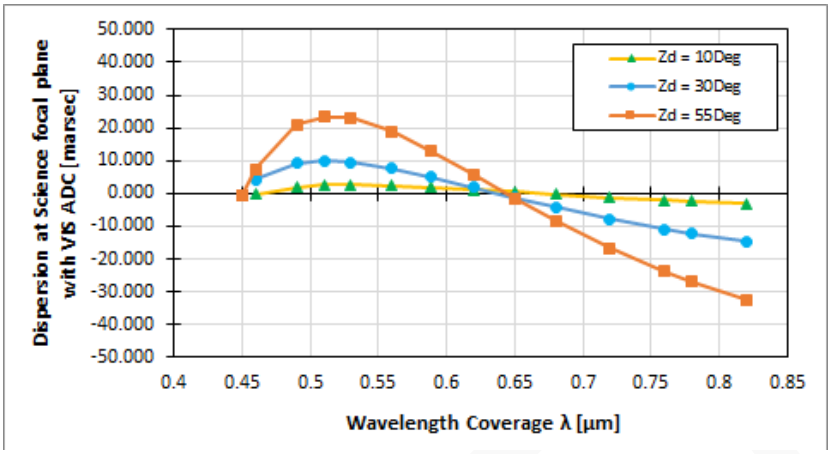

Figure 32: Residual Chromatic dispersion as a function of wavelengths for three telescope elevations. Yellow: Zd 10Deg. elevation; Blue: Zd 30Deg. elevation; Orange: Zd 55Deg. elevation. ADC Rotation angle is 83Deg., 67Deg. and 18Deg.

The estimated throughput (see Table 5) at the NGS focal plane is 84% at 0.6um with protected silver coating for reflective optics (R ~ 99%) and AR coating for the refractive optics (T ~ 96% for BS). The estimated throughput of the ADC is 98.2% at 0.6um and 93.86% at 0.45um.

Table 5: NGS Throughput with VIS ADC

number of element	Optics	Coating	T@0.6um	T@0.45um
1	FM	Protected Silver	99.00	99.00
2	SM1	Protected Silver	99.00	99.00
3	FM	Protected Silver	99.00	99.00
4	DM0	Protected Silver	99.00	99.00
5	SM2	Protected Silver	99.00	99.00
6	SM3	Protected Silver	99.00	99.00
7	Science BS	SILICA + NIR AR Coating	96.00	96.00
8	LGS BS	SILICA + Coating	96.00	96.00
9	FM	Protected Silver	99.00	99.00
10	NGS ADC	VIS GLASS	98.21	93.86
Total	AO bench NGS Path		84.36	80.63

The optical specifications of Table 2 are met by the MOC relay design in the VIS domain. The relay is near diffraction-limited over the field-of-view. Optical distortion is reduced by a factor of 4 compared to the OAP relay. Chromatic shift at the focal plane due to the lack of collimated space can be problematic.

DRAFT

2.2 Off-axis Parabolas relay

2.2.1 Science Performance

The following section shows the optical performance of the OAP relay in the NIR domain at 1.65um. Figure 34 shows the spot diagram over the field-of-view and the static optical distortion. As it can be seen the spot is included in the Airy disk over the entire field. Optical distortion at the science focal plane is <1.9% on average. Figure 35 shows the Point Spread Function (PSF) at 1.65um on-axis and off-axis. PSF is 99.9% on-axis and 95.8% off-axis with a maximum variation of 4.2% over the field.

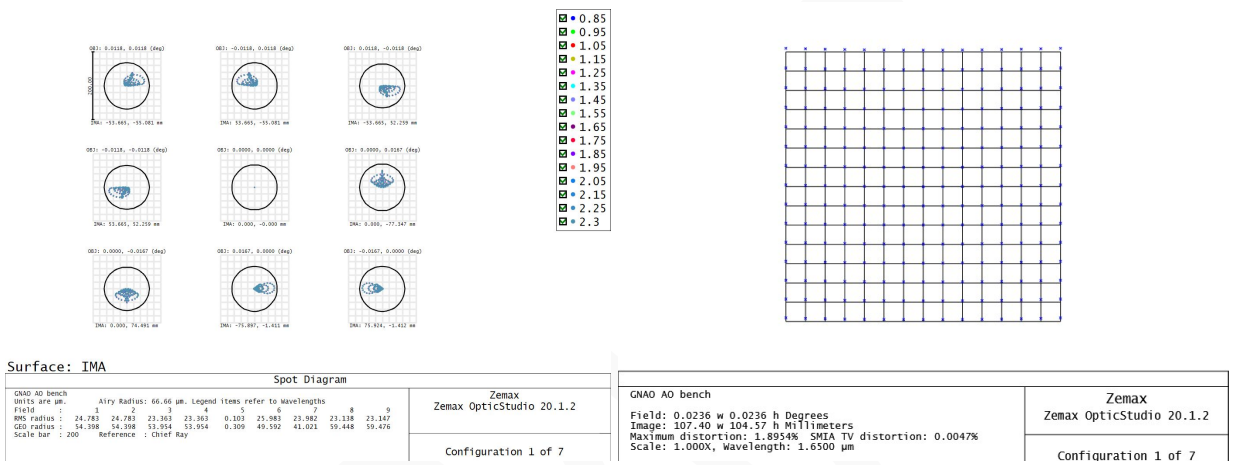

Figure 34: Spot Diagram at left and Static distortion at right. Central spot: on-axis field; Other spots: Off-axis fields at 1 arcmin radius from the center.

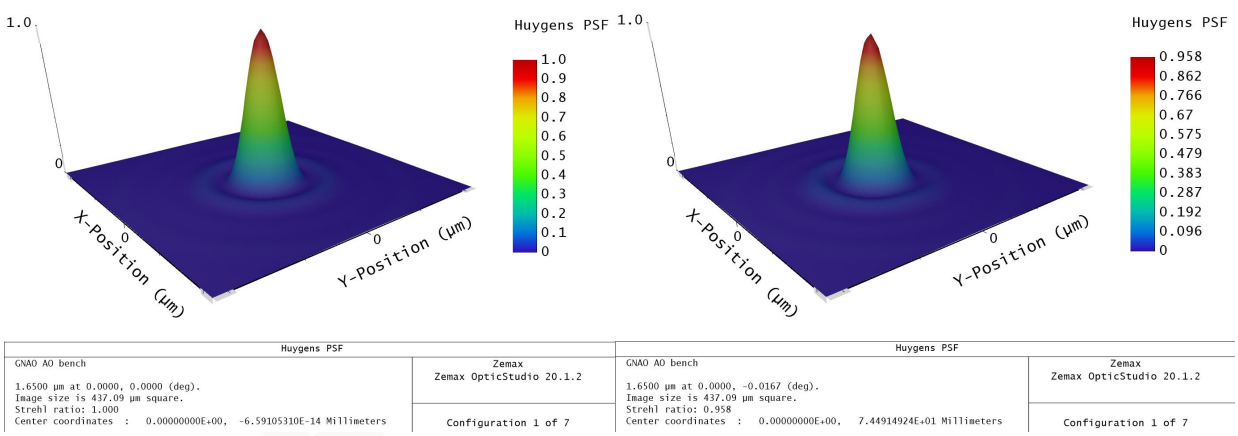

Figure 35: Point Spread Function on-axis at left and for the worst performing field off-axis at right. Strelh ratio is 99% on-axis and 95.8% off-axis.

Figure 36 shows the Sagittal and Tangential field curvature in +Y and +X as a function of the field size. Figure 37 shows the polychromatic RMS WaveFront error in +Y and +X as a function of the field size. In both Figures, performance in -Y and -X are not shown for similarity. It can be seen that Field Curvature is less than 2mm on average at the edge of the field. Regarding RMS WFE

error, it is shown the OAP relay is diffraction-limited for all the wavelengths in the NIR domain from 0.83 to 2.5um and over the entire Field-of-view.

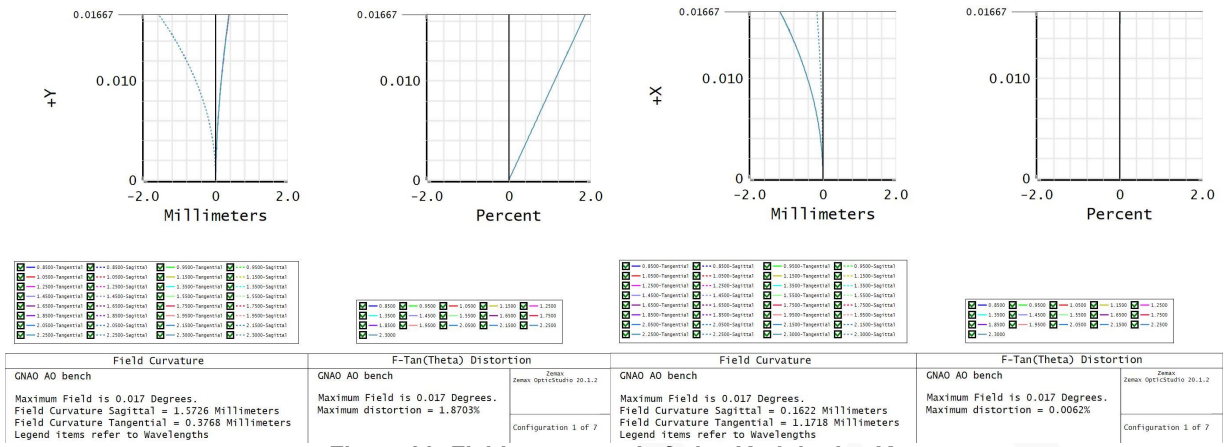

Figure 36: Field curvature. Left: in +Y; right: in +X.

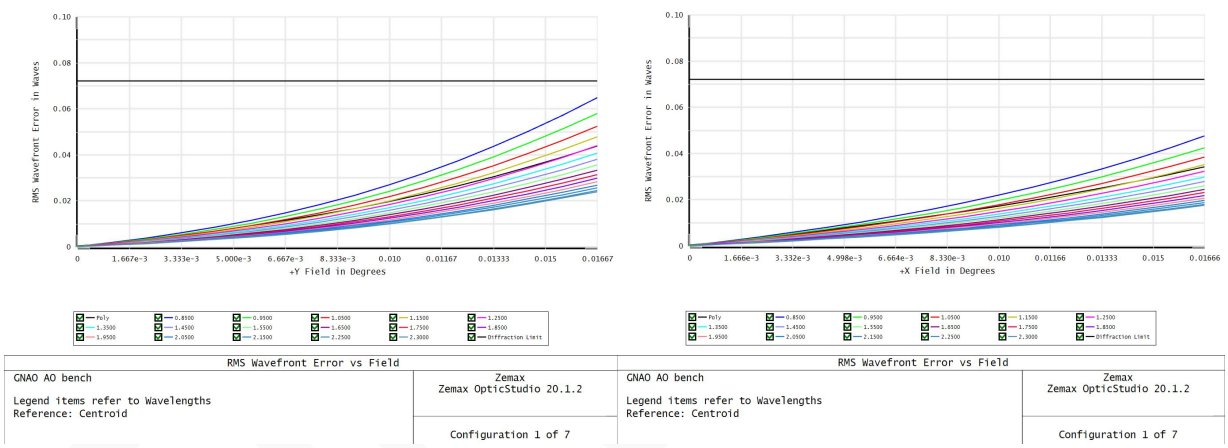

Figure 37: RMS WFE as a function of Field in +Y and +X at left and right. each color for each wavelength. Black line is diffraction-limited.

Figure 38 shows the wave front map for the on-axis field and the worst performing off-axis field at a wavelength of 1.65um. RMS WFE is 1nm on-axis and 55nm off-axis. The requirement of 60nm RMS for wave front error is met over the entire field but the goal of 40nm will not be achieved at the edge of the field due to the effect of third-order aberrations.

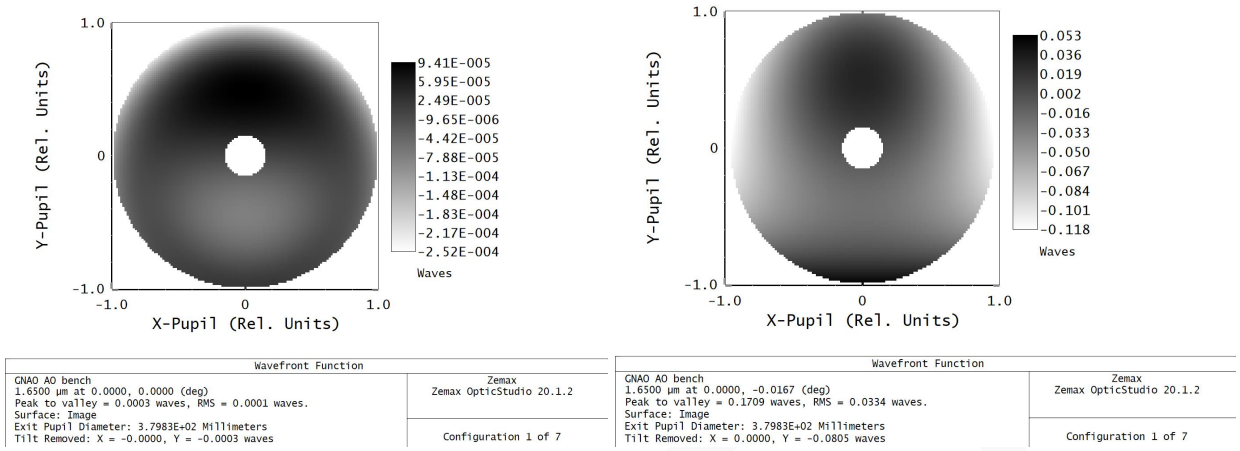

Figure 38: Wave front Map on-axis at left off-axis at right at 1.65um.

The reflective design of the OAP relay does not produce chromatic aberration at the science focal plane. The refractive optics in the OAP relay are located in the collimated space that brings some advantage in terms of chromaticity compared to the MOC relay. The glass material for the BS is SILICA for the high transmittance in the NIR wavelength coverage. Figure 39 shows the Lateral and longitudinal color.

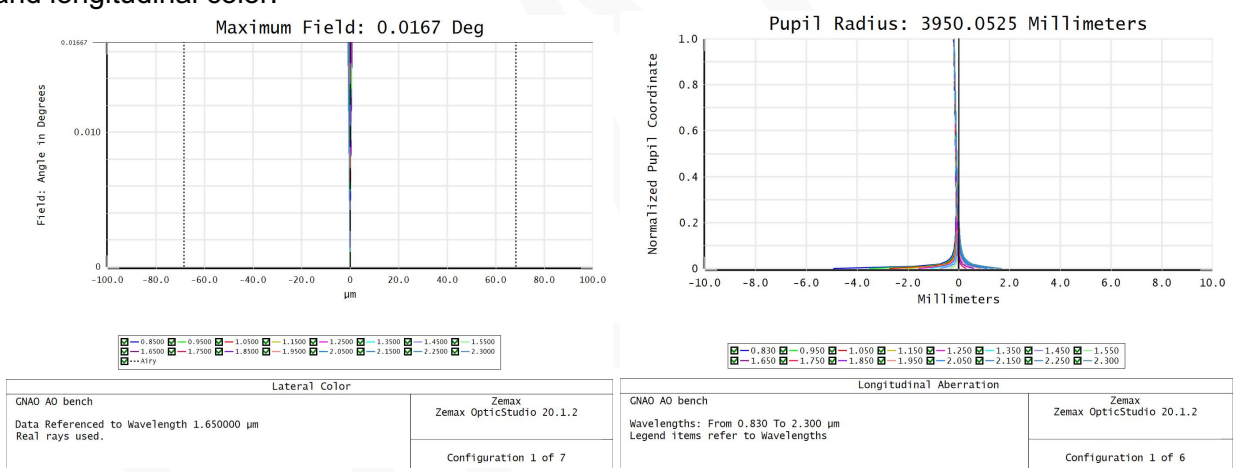

Figure 39: Lateral and longitudinal color as a function of field. each color for each wavelength.

No significant amount of lateral color and longitudinal color is seen at the science focal plane with wavelengths. The chromatic shift is lower than 10um over the NIR domain which is negligible compared to the MOC relay (Figure 40).

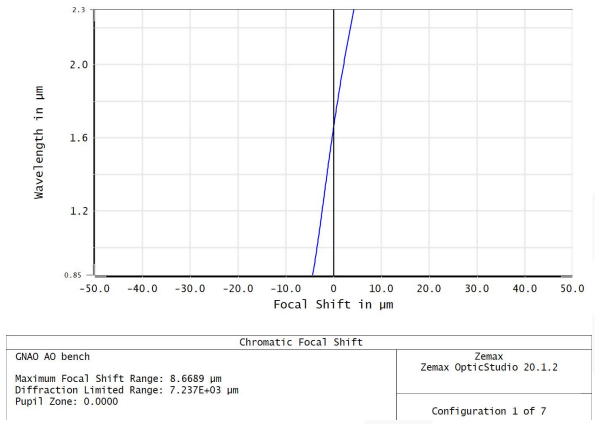

Figure 40: Chromatic shift at the science focal plane as a function of wavelengths in the NIR Domain.

Regarding residual chromatic dispersion at the science focal plane, no detail is provided in this section for similarity with section 2.1.1.

The estimated throughput of the science path without ADC is 90% at 1.65um with protected silver coating for reflective optics (R ~ 99%) and AR coating for the refractive optics (T ~ 96% for BS).

Table 6: Science Throughput

number of element	Optics	Coating	T@1.65um	T@2.2um in K-band
1	FM	Protected Silver	99.00	99.00
2	OAP1	Protected Silver	99.00	99.00
3	FM/DMx	Protected Silver	99.00	99.00
4	DM0	Protected Silver	99.00	99.00
5	FM/TTM	Protected Silver	99.00	99.00
6	BS	Protected Silver	96.00	96.00
7	ADC	Protected Silver	TBD	TBD
8	OAP2	SILICA + NIR AR Coating	99.00	99.00
9	FM	Protected Silver	99.00	99.00
		r		
Total	AO bench w/o ADC		90.00	90.00

The optical specifications of Table 1 are met by the OAP relay design in the NIR domain. The relay is diffraction-limited over the entire field-of-view and the NIR spectral range. Strehl ratio is better than 95% with a variation below 4%, which means the performance uniformity is worse than the Offner relay. Optical static optical distortion is about 1.8% on average that is similar to CANOPUS distortion but it can be slightly improved by re-optimizing the OAP relay. Distortion less than 1.5% will not be achieved in an OAP relay considering the little space for the optics. The goal of 40nm RMS is almost achieved at the science focal plane except at the edge of the field due to third-order aberrations and especially astigmatism. The focus shift with wavelengths is negligible and no residual chromatic aberration is introduced by the refractive optics thanks to the collimated space.

2.2.1 WFS Performance

The following section shows the optical performance of the MOC relay in the VIS domain at 0.6um for the NGS path. Figure 41 shows the spot diagram over the field-of-view and the static grid distortion. As it can be seen the spot is near the diffraction-limited. The optical distortion at the NGS focal plane is <1.6% on average. Compromise is found in which the NGS off-axis relay provides a telecentric beam, a focal ratio near to f/16 and a strehl ratio better than 0.7% over the field. Figure 42 shows the Point Spread Function (PSF) at 0.6um on-axis and off-axis. PSF is 79% on-axis and 96.6% off-axis.

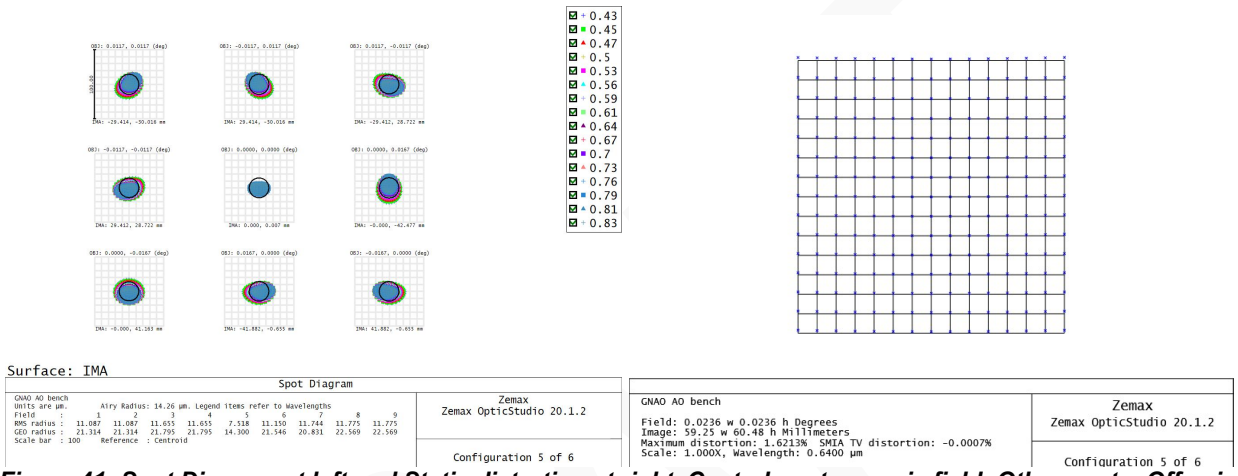

Figure 41: Spot Diagram at left and Static distortion at right. Central spot: on-axis field; Other spots: Off-axis fields at 1 arcmin radius from the center.

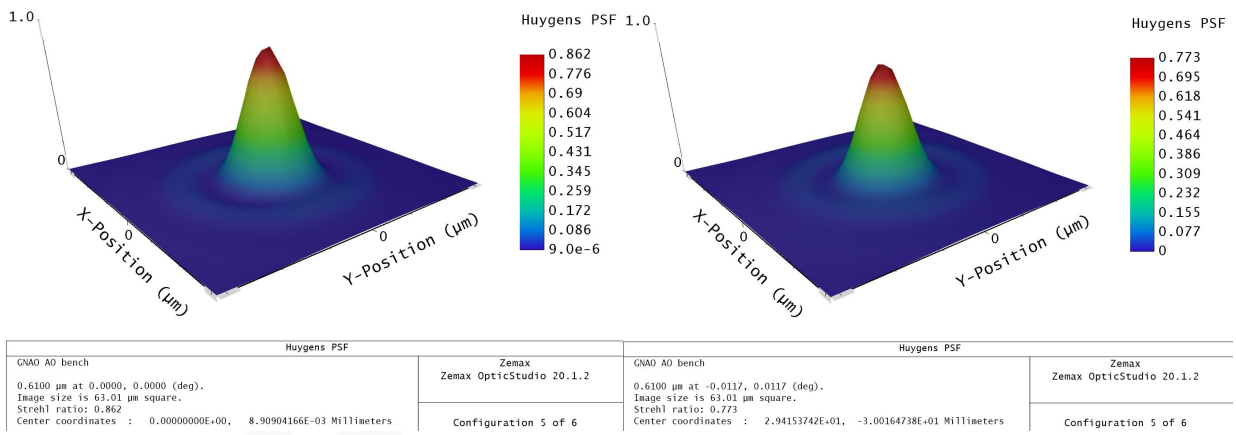

Figure 42: Point Spread Function on-axis at left and for the worst performing field off-axis at right. Strelh ratio is 86% on-axis and 77% off-axis.

Figure 43 at left shows the Sagittal and Tangential field curvature in +Y as a function of the field size and Figure 43 at right shows the polychromatic RMS WaveFront error in +Y as a function of the field size. In both Figures, performance in -Y and -X are not shown for similarity. It can be seen that Field Curvature is less than 2mm on average at the edge of the field. Regarding RMS

WFE error, it is shown the MOC relay is near diffraction-limited for all the wavelengths in the VIS domain from 0.45 to 0.83um on-axis but degradation of image quality takes place off-axis.

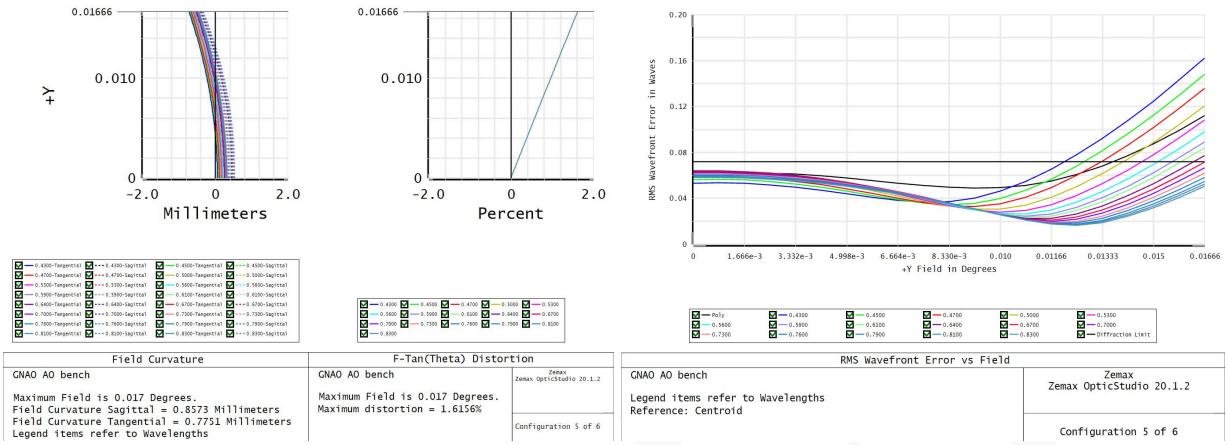

Figure 43: Field Curvature in +Y and RMS WFE in +Y as a function of Field.

Figure 44 shows the wave front map for the on-axis field and the worst performing off-axis field at a wavelength of 0.6um. RMS WFE is 38nm on-axis and 50nm off-axis.

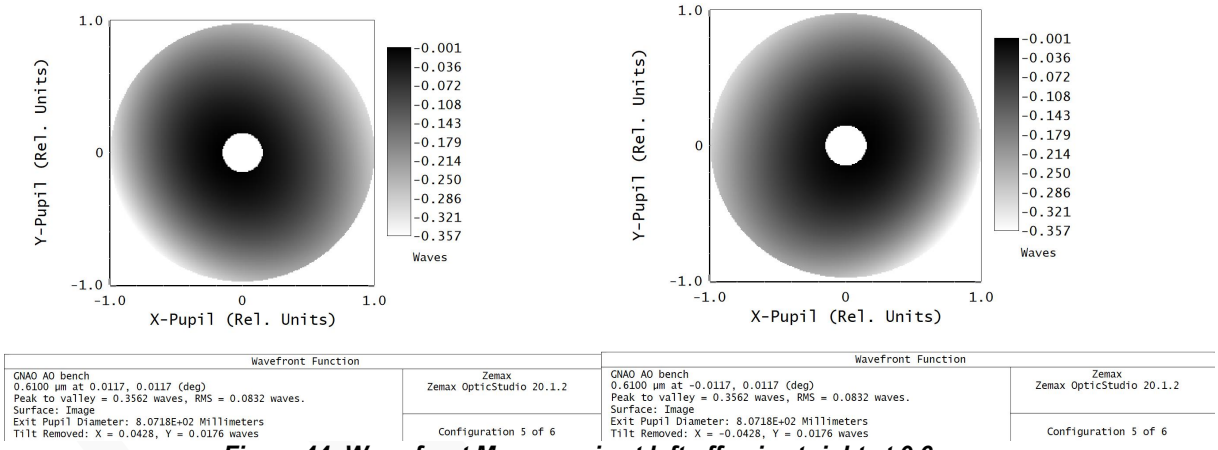

Figure 44: Wave front Map on-axis at left off-axis at right at 0.6um.

The reflective design of the MOC relay does not produce chromatic aberration at the WFS focal plane. Chromatic aberration is produced by the LGS BS due to its location in the converging beam. Figure 45 shows the Lateral and Longitudinal color at the NGS focal plane.

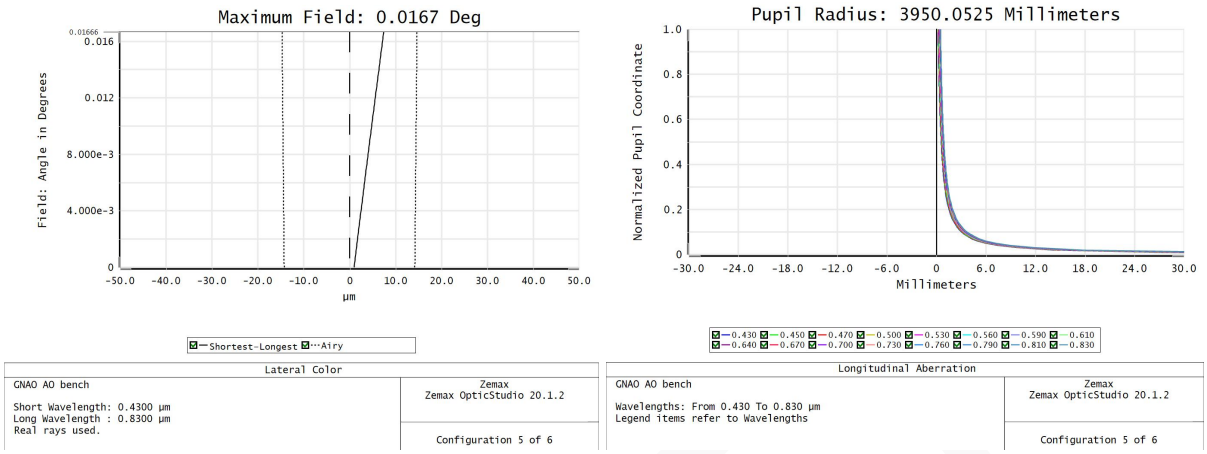

Figure 45: Lateral and Longitudinal aberration as a function of field. each color for each wavelength.

The chromatic aberration produces a chromatic shift of 0.200mm from 0.45 to 0.83um.

The estimated throughput (see, Table 6) at the NGS focal plane is 86% at 0.6um with protected silver coating for reflective optics (R ~ 99%) and AR coating for the refractive optics (T ~ 96% for BS). The throughput of the ADC is 98.2% at 0.6um and 93.86% at 0.45um.

Table 7: NGS Throughput

number of element	Optics	Coating	T@0.6um	T@0.45um
1	FM	Protected Silver	99.00	99.00
2	OAP1	Protected Silver	99.00	99.00
3	FM	Protected Silver	99.00	99.00
4	DM0	Protected Silver	99.00	99.00
5	TTM	Protected Silver	99.00	99.00
6	Science BS	SILICA + NIR AR Coating	98.00	98.00
7	OAP3	SILICA + Coating	99.00	99.00
8	FM	Protected Silver	99.00	99.00
9	LGS BS ADC	SILICA + VIS AR Coating	96.00	96.00
10	NGS ADC	VIS GLASS	98.21	93.86
Total	AO bench NGS Path		86.12	82.30

The optical specifications of table 2 are met by the OAP design in the VIS domain. The relay is near diffraction-limited over the entire field-of-view. Optical distortion is 1.6%. Chromatic shift at the NGS focal plane due to the lack of collimated space can be problematic since a focus shift with wavelength is seen in the VIS. Throughput is about 86% with ADC.

DRAFT

3. Tolerancing analysis

Table 8 shows a list of manufacturing and mounting tolerances and ranges used to perform an analysis of the image quality degradation with a Monte Carlo approach. The tolerancing criterion for a diffraction-limited system is RMS wave front. Back focal length compensation of ±4mm is allowed at the focal plane. Analysis is performed at a wavelength of 1.65μm for the science path only. Sensitivity analysis gives the worst offenders in each case and the estimated change of WFE RMS.

Table 8: Set of standard manufacturing and mounting tolerances and ranges for AO.

Tolerances	Optics	Ranges	Unit
Manufacturing			
Radius of Curvature	Spherical Mirrors and Off-axis parabolas	±2	[%]
Flatness	Fold Mirrors, Deformable mirrors, Beam Splitter	±0.5	Fringes
Irregularity	all optics	±0.2	Fringes
Conic Constant	Off-axis parabolas	±0.001	Unitless
Refraction Index	Beam splitter	±0.001	Unitless
Abbe number	BS	±0.01	Unitless
Wedge	BS	±0.05	[mm]
Mounting			
Thickness	all optics	±0.2	[mm]
Decenter X/Y	all optics	±0.2	[mm]
Tilt X/Y	all optics	±0.005	[Deg]
Off-axis angle	OAP	±0.001	[Deg]

3.1 Modified Offner Concentric relay

To illustrate the MOC relay image quality degradation with tolerances, Figure 46 shows the nominal performance at left, and performance considering standard manufacturing and mounting tolerances at right. The nominal criterion is 0.029 wave or 48nm RMS.

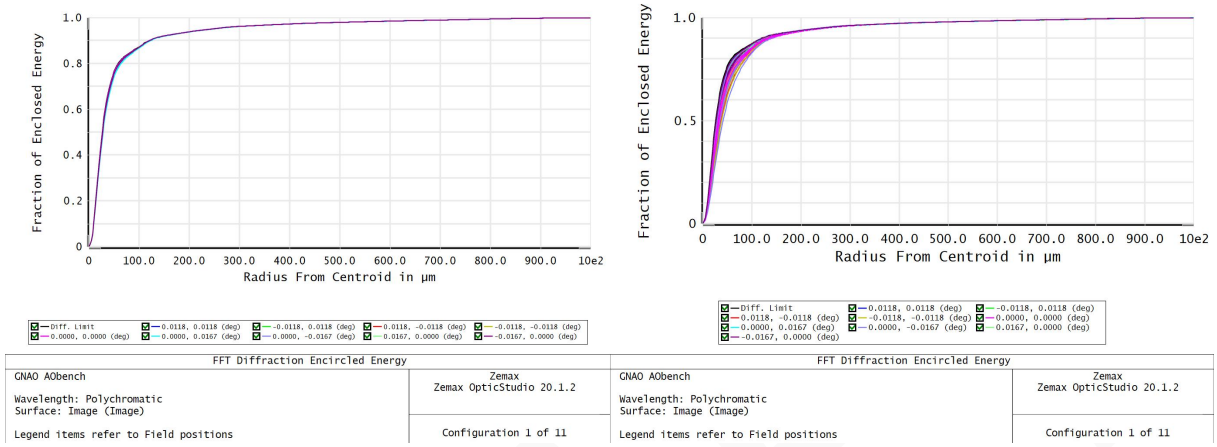

Figure 46: MOC relay Image degradation with standard mounting and manufacturing tolerances. Left: Nominal performance. Right: considering tolerances of table 8.

The sensitivity analysis shows errors of the radius of curvature (TRAD) of the three spherical mirrors are the worst offenders followed by tilt and wedge angle of the beam splitter (TIRY/TIRX). The estimated change of WFE is 0.020 wave or 32nm RMS on average. From the Monte Carlo approach, the estimated change is 0.017 wave RMS (28nm) on average with a standard deviation of 0.015 wave. In the worst case the maximum degradation is 0.067 wave or 110nm RMS.

Worst offenders:

Type			Value	Criterion	Change
TRAD	24	1	0.20000000	0.07167410	0.04190809
TRAD	38	1	0.20000000	0.06151834	0.03175233
TRAD	35	1	-0.20000000	0.05786567	0.02809966
TIRR	21		0.20000000	0.03699509	0.00722908
TIRY	46		0.05000000	0.03662627	0.00686026
TIRY	46		0.05000000	0.03662627	0.00686026
TIRR	42		0.20000000	0.03661065	0.00684464
TIRY	48		-0.05000000	0.03656193	0.00679592
TIRY	48		-0.05000000	0.03656193	0.00679592
TIRX	46		0.05000000	0.03575592	0.00598991

List of worst offenders

3.2 Off-axis Parabola relay

To illustrate the OAP image quality degradation with tolerances, Figure 47 shows the nominal performance at left, and performance considering standard manufacturing and mounting tolerances at right. The nominal criterion is 0.026 wave or 43nm RMS.

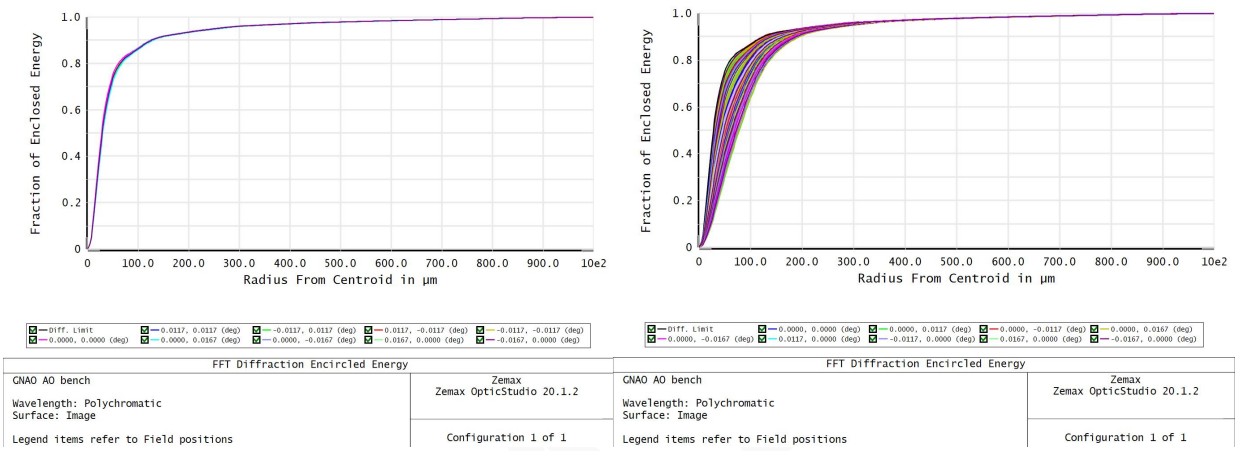

Figure 47: OAP relay Image degradation with standard mounting and manufacturing tolerances. Left: Nominal performance. Right: considering tolerances of table 8.

The analysis shows errors of the radius of curvature (TRAD) of the two off-axis parabolas are the worst offenders followed by surface irregularity and flatness of the deformable mirrors (TFRN and TIRR). The estimated change of WFE is 0.10 wave or 132nm RMS. From the Monte Carlo approach, the estimated change is 0.044 wave RMS (72nm) on average with a standard deviation of 0.037 wave. In the worst case the maximum degradation is 280nm RMS.

Worst offenders:

Type			Value	Criterion	Change
TRAD	23	1	0.20000000	0.10289189	0.07650288
TRAD	41	1	-0.20000000	0.08858618	0.06219717
TRAD	23	1	-0.20000000	0.08626273	0.05987372
TFRN	31		0.50000000	0.07537325	0.04898424
TRAD	41	1	0.20000000	0.07276549	0.04637648
TFRN	31		-0.50000000	0.06085181	0.03446280
TIRR	31		0.20000000	0.06075348	0.03436447
TIRR	31		-0.20000000	0.05762214	0.03123313
TFRN	27		-0.50000000	0.04746854	0.02107953
TIRY	37		-0.05000000	0.04403171	0.01764271

List of worst offenders

This analysis suggests the effect of manufacturing and mounting errors on image quality is worse in the OAP relay. In both relays the degradation of image quality is mainly due to manufacturing errors of powered optics. In the MOC relay, tilt misalignment of the BS in converging beams can affect the image quality. Tilt and decentration of other optics have only a minor impact on image quality degradation. In the OAP relay, tilt misalignment of refractive optics in collimated space has

no effect compared to the MOC relay. However, decentration and tilt misalignments of other optics in the train have a major impact on image quality degradation since the alignment with OAP off-axis angle is critical.

DRAFT

4. Discussion

In this document two optical concepts based on a MOC relay and an OAP relay have been studied for the AO bench. Both concepts can be implemented to reimage the telescope f/16 focal plane to the science focal plane with diffraction-limited image quality in the NIR domain. Both conceptual designs produce an optical plane for a deformable mirror with a diameter of 85 mm.

In terms of performance, the MOC relay has the main advantage of producing a focal plane with less aberrations than the OAP relay. Static optical distortion is reduced by a factor of 4 compared to the OAP baseline. Petzval field curvature can be compensated while astigmatism and coma are minimized. In an OAP relay the aberrations cannot be balanced at the image plane.

Regarding the image quality both designs perform well producing diffraction-limited image quality in the NIR spectral range for a circular field-of-view of 2 arcmin diameter. The science PSF is better than 95% over the 2 arcmin FoV with a variation below 2% for the MOC relay while it is about 4.5% for the OAP which means uniformity of the PSF over the field is improved with the MOC relay.

The reflective design does not produce chromatic aberration and the dispersion introduced by the atmosphere can be corrected with the implementation of an ADC. Nonetheless, the lack of collimated space in the MOC results in a slight increase of longitudinal chromatic aberration that is not seen in the OAP relay.

Both optical layouts have the same number of optical components in the optical train with an estimation of throughput of approximately 89%.
Regarding optical performance in the VIS spectral range, the same conclusions are made. The MOC relay provides slightly better performance than OAP but the lack of collimated beam remains the main disadvantage by introducing higher chromatic aberration in the VIS and a focus shift at the NGS focal plane.

In terms of manufacturability and cost, custom OAPs are more expensive and difficult to fabricate than custom spherical mirrors which means the cost of the MOC relay is less expensive and easier to build. Optics size in both designs is standard for astronomical instruments. Another advantage of spherical mirrors is the optical alignment compared to OAP.

Regarding dimensioning, the OAP relay brings significant advantages in terms of compactness and size compared to the MOC with additional space for the WFS. Alternative optical layouts can be further studied to optimize space with different folding options.

The tolerancing analysis shows the MOC relay is also a robust optical system less sensitive to optical misalignment than OAP that is much more sensitive to the off-axis angle misalignment. Standard tolerances (decentration and tilt of the optics) have only a minor impact on the image quality degradation compared to OAP that bring great advantages for a system operating in a gravity variant environment as it is at GN.

In conclusion, both designs based on the MOC relay and the OAP relay can be implemented for the GNAO bench design with their own advantages and drawbacks. The MOC relay provides better optical performance, robustness at a lower cost than OAP. The advantages of the OAP are essentially related to the accessibility of collimated space for the refractive optics (ADC and BS), the compactness for the WFS and the well-known approach in AO instrumentation.

- To build an AO bench with enhanced performance (optical distortion, PSF homogeneity, balancing of third-order aberration), the *MOC relay* is an interesting alternative to off-axis parabolas but it can be difficult to implement in the required space.

- To build an AO bench with identical optical performance as CANOPUS, *OAP relay* is the design to implement for simplicity.

DRAFT

Acronyms and Abbreviations

Acronym	Meaning
ADC	Atmospheric Dispersion Corrector
ASM	Adaptive Secondary Mirror
AO	Adaptive Optics
BS	Beam Splitter
DM	Deformable Mirror
FoV	Field-of-View
FM	Fold Mirror
GNAO	Gemini North Adaptive Optics
GLAO	Ground Layer Adaptive Optics
LGS	Laser Guide Star
LTAO	Laser Tomography Adaptive Optics
MLA	Micro-Lens Array
MOC	Modified Offner Concentric
NGS	Natural Guide Star
NIR	Near InfraRed
OAP	Off-Axis Parabolas
R	Reflectance
SH WFS	Shack-Hartmann Wave Front Sensor
SFS	Slow Focus Sensor
SM	Spherical Mirror
T	Transmittance
TTM	Tip-Tilt Mirror
VIS	Visible
WFS	Wave Front sensor

DRAFT